Free Electron Lasers

Lecture IV

Brian M^{c}Neil,
University of Strathclyde,
Glasgow, Scotland.

Spoiling effects

Energy spread

The effects of energy spread can be investigated by introducing a spread in the initial values of p_j :

$$\delta_j = p_j\left(\bar{z}=0\right) \equiv \frac{\gamma_r - \gamma_j\left(\bar{z}=0\right)}{\rho\,\gamma_r}$$

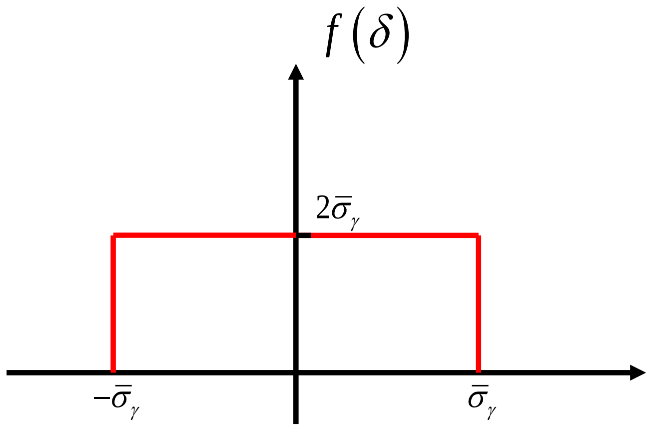

The steady state dispersion relation becomes:

$$\lambda - \int_{-\infty}^{\infty} \frac{\mathrm{d}\delta\, f(\delta)}{(\lambda-\delta)^2} = 0$$

with solutions for the imaginary part of lambda, determining the high gain case, shown opposite. Energy spread effects become less important when:

$$\bar{\sigma}_\gamma < 1 \quad \Rightarrow \quad \frac{\sigma_\gamma}{\gamma} < \rho$$

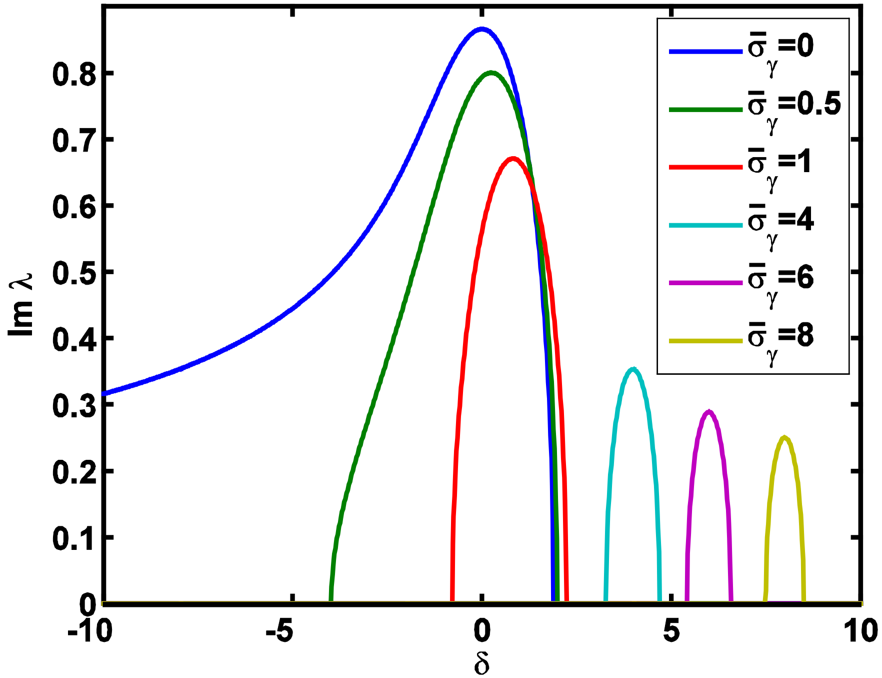

R. Bonifacio [1], L. De Salvo Souza and B.W.J. McNeil Optics Communications 93 (1992) 179–185

Emittance*

The beam emittance introduces two main effects:

1) The electron beam radius in a matched focussing channel** is determined by the emittance via:

$$r_b = \sqrt{\frac{\varepsilon_n \beta}{\gamma}} \Rightarrow \rho = \left(\frac{e}{16\pi\epsilon_0 m c^3} \frac{I_{pk} a_w^2 f_B^2}{\gamma_r^2 k_w^2 \epsilon_n \beta} \right)^{1/3}$$

β – betafunction of focussing lattice.

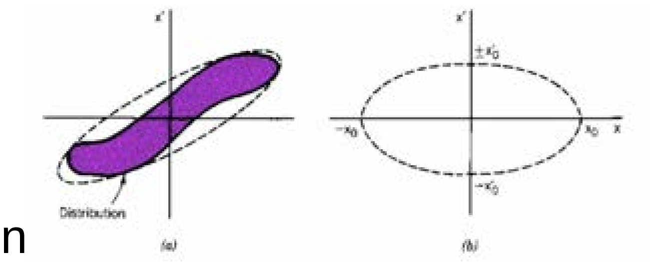

Figure 3.8. Definition of emittance. (a) Uniform orbit-vector distribution inside a boundary, surrounded by a minimum-area ellipse. (b) Upright trace-space ellipse — the enclosed emittance equals $x_0 x_0'$ π-m-rad.

2) The emittance introduces an energy spread in the resonant electron energy***. This can be added in quadrature with the real energy spread to estimate emittance effects in a 1D model:

$$\sigma_\epsilon = \frac{\epsilon_n a_w^2 k_w^2 \beta}{4\gamma_r (1 + a_w^2)} \Rightarrow \sigma_{eff} = \sqrt{\sigma_\epsilon^2 + \sigma_\gamma^2}.$$

$$\Rightarrow \frac{\sigma_{eff}}{\gamma} < \rho$$

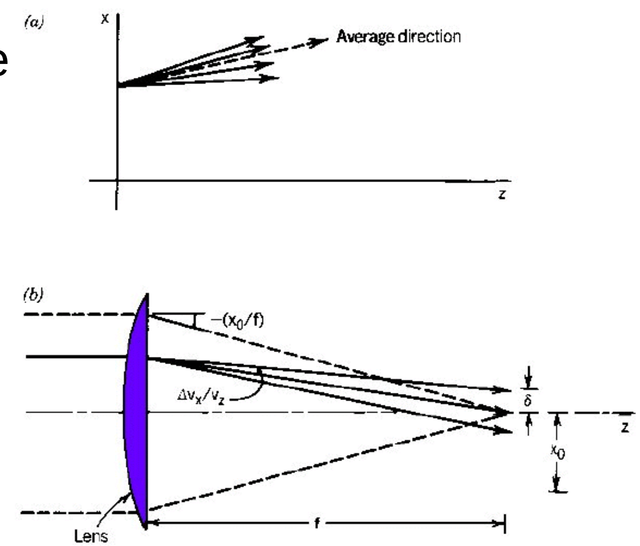

***Stanley Humphries,Charged Particle Beams:** http://www.fieldp.com/cpb.html

**See H. Owen course

***R. Bonifacio [1], L. De Salvo Souza and B.W.J. McNeil Optics Communications 93 (1992) 179–185

Diffraction

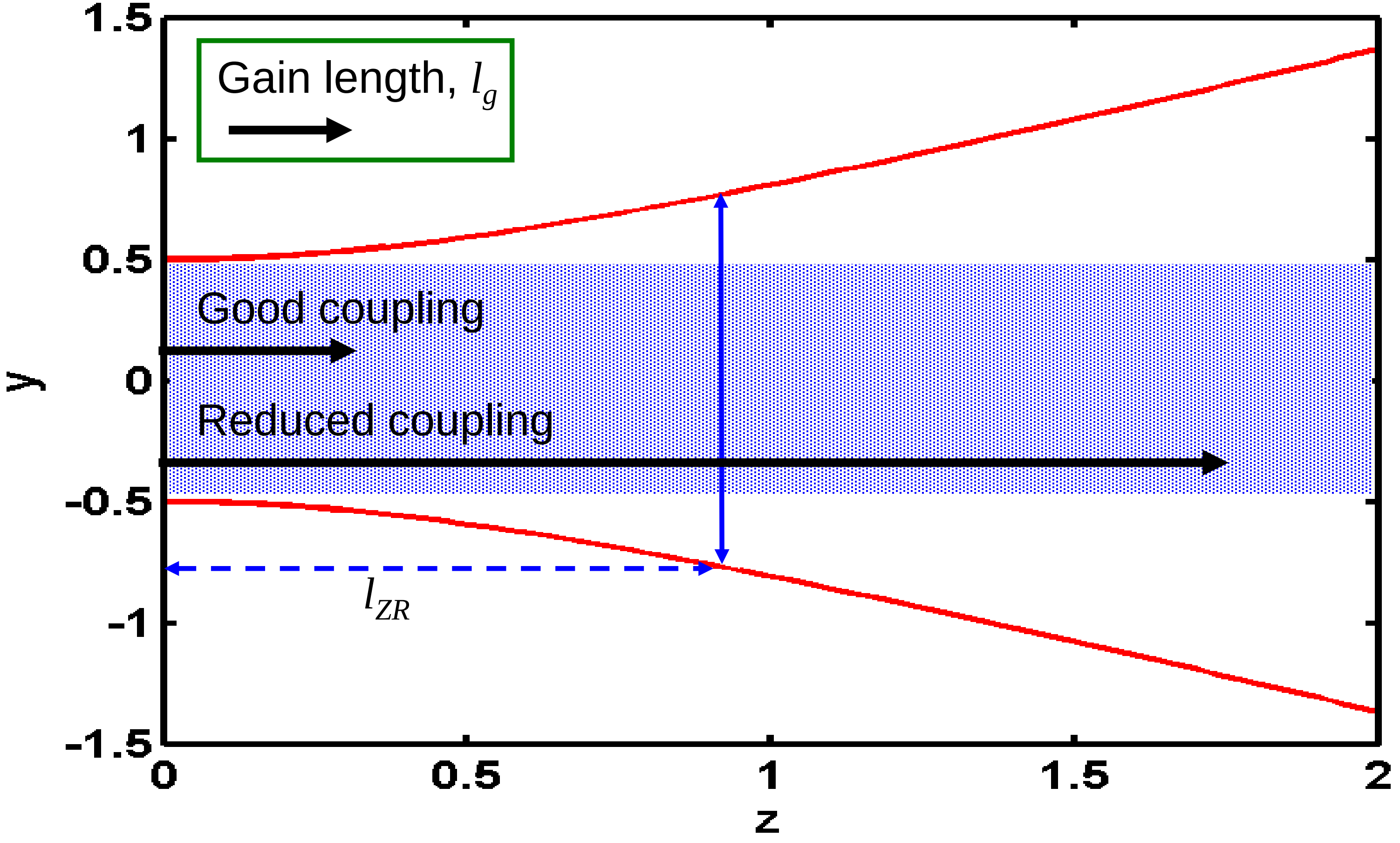

The Rayleigh length l_{ZR} is that in which a beam diffracts to twice its transverse mode area. In an FEL amplifier, if the gain length of the FEL interaction is greater than the Rayleigh length then diffraction can cause reduced coupling and longer saturation lengths.

8.1.3.3 Summary of Criteria for Optimum FEL Performance*

The one-dimensional theory describes the best-case limit for FEL operation. The following summarises the limits required for the one-dimensional equations to be a valid approximation for a high gain FEL interaction that achieves saturation:

- $L_u \gg L_g$ - The undulator is significantly longer than the interaction gain length
- $L_g \lesssim l_{ZR}$ - The gain length is less than the Rayleigh range
- $L_g < \beta$ - The gain length is less than the betatron function
- $\delta_r \ll r_b$ - Electron beam wander off-axis is much less than the beam radius
- $r_b \approx$ constant - The electron beam radius is approximately a constant
- $\sigma_\gamma \lesssim \rho$ - Homogeneous relative energy spread is less than the FEL coupling parameter
- $\sigma_\varepsilon \lesssim \rho$ - Resonant relative energy spread due to emittance is less than the FEL coupling parameter

*4GLS Conceptual Design Report, Chapter 8: http://www.4gls.ac.uk/documents.htm

Real FEL designs as taken from the 4GLS design*

*4GLS Conceptual Design Report, Chapter 8: http://www.4gls.ac.uk/documents.htm

4GLS CDR – April 2006

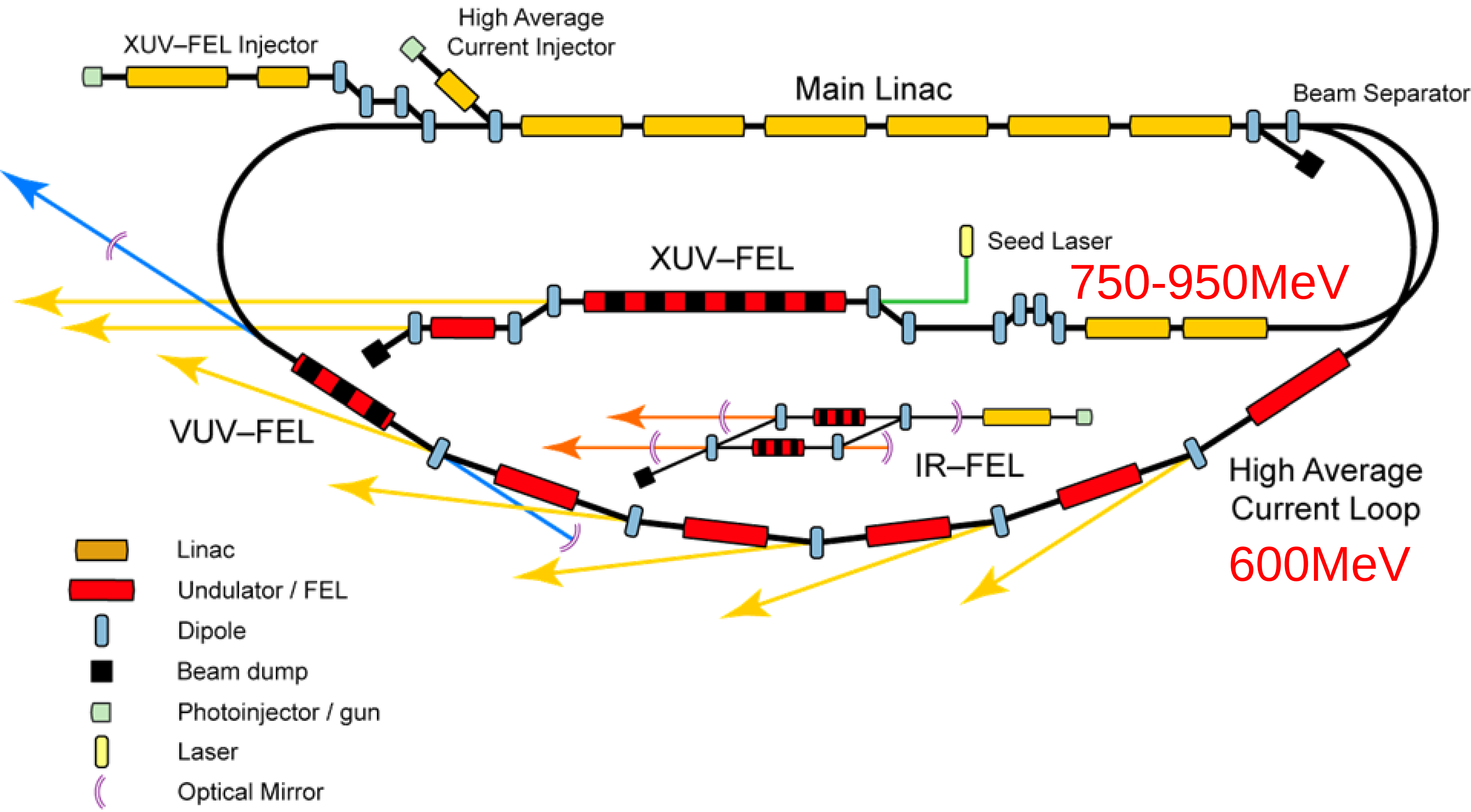

Table 8.1 Summary of parameter and performance estimates for the FEL sources of 4GLS

	XUV-FEL	*VUV-FEL*	*IR-FEL*
FEL DESCRIPTION			
FEL design	High Gain Amplifier	Regenerative Amplifier	Oscillator
Seeding type	External seeding	Self-seeding	Self-seeding
Seeding mechanism	HHG source	Low-Q cavity	High-Q cavity
FEL PHOTON OUTPUT			
Tuning Range	8 - 100 eV	3 - 10 eV	2.5 - 200 μm
Repetition rate	1 kHz	n × 4⅓ MHz	13 MHz
Polarisation	Variable elliptical	Variable elliptical	Variable elliptical
Max Peak Power	8 GW	500 MW (3 GW*)	9 MW (>20 MW*)
Pulse length FWHM	< 50 fs	170 fs (25 fs*)	2 ps (300 fs*)
Typical $\Delta\nu\Delta t$	≈ 0.6	≈ 1.0	≈ 0.9
Max pulse energy	400 μJ	70 μJ	50 μJ
ELECTRON BEAM PARAMETERS AT FEL			
Energy	750 - 950 MeV	600 MeV	25 - 60 MeV
Bunch Charge	1 nC	77 pC	200 pC
RMS bunch length	266 fs	100 fs	1 - 10 ps
Peak Current	1.5 kA	300 A	8 - 80 A
Normalised emittance	2 mm mrad	2 mm mrad	10 mm mrad
RMS energy spread	0.1 %	0.1 %	0.1 %
UNDULATOR PARAMETERS			
Undulator Type	PPM & APPLE-II	APPLE-II	APPLE-II
No of Modules	8 & 5	5	1 & 1
Module length	2 m	2.2 m	2.65 m & 5.07 m
Period	45 mm & 51 mm	60 mm	53 mm & 145 mm
Focussing	FODO	FODO	Natural
Minimum magnetic gap	10 mm	10 mm	23.5 mm & 74 mm

* indicates possible output in superradiant mode

New Journal of Physics
The open-access journal for physics

New Journal of Physics 9 (2007) 82

An XUV-FEL amplifier seeded using high harmonic generation

B W J McNeil[1,5], J A Clarke[2], D J Dunning[2], G J Hirst[3], H L Owen[2], N R Thompson[2], B Sheehy[4] and P H Williams[2]

New Journal of Physics
The open-access journal for physics

New Journal of Physics 9 (2007) 239

A design for the generation of temporally-coherent radiation pulses in the VUV and beyond by a self-seeding high-gain free electron laser amplifier

B W J McNeil[1,4], N R Thompson[1,2], D J Dunning[2], J G Karssenberg[3], P J M van der Slot[3] and K-J Boller[3]

XUV-FEL (~10-100nm)

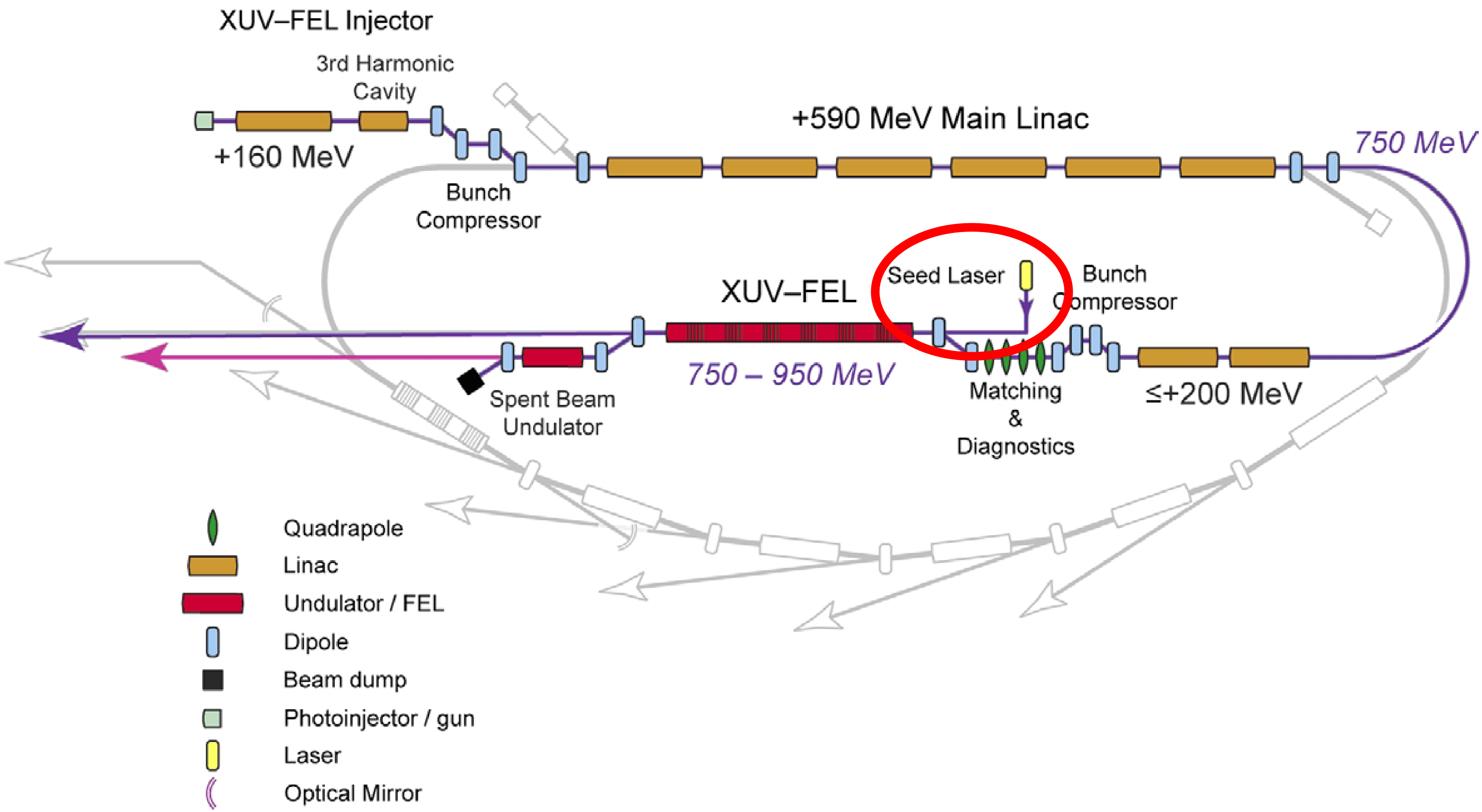

HHG seed sources

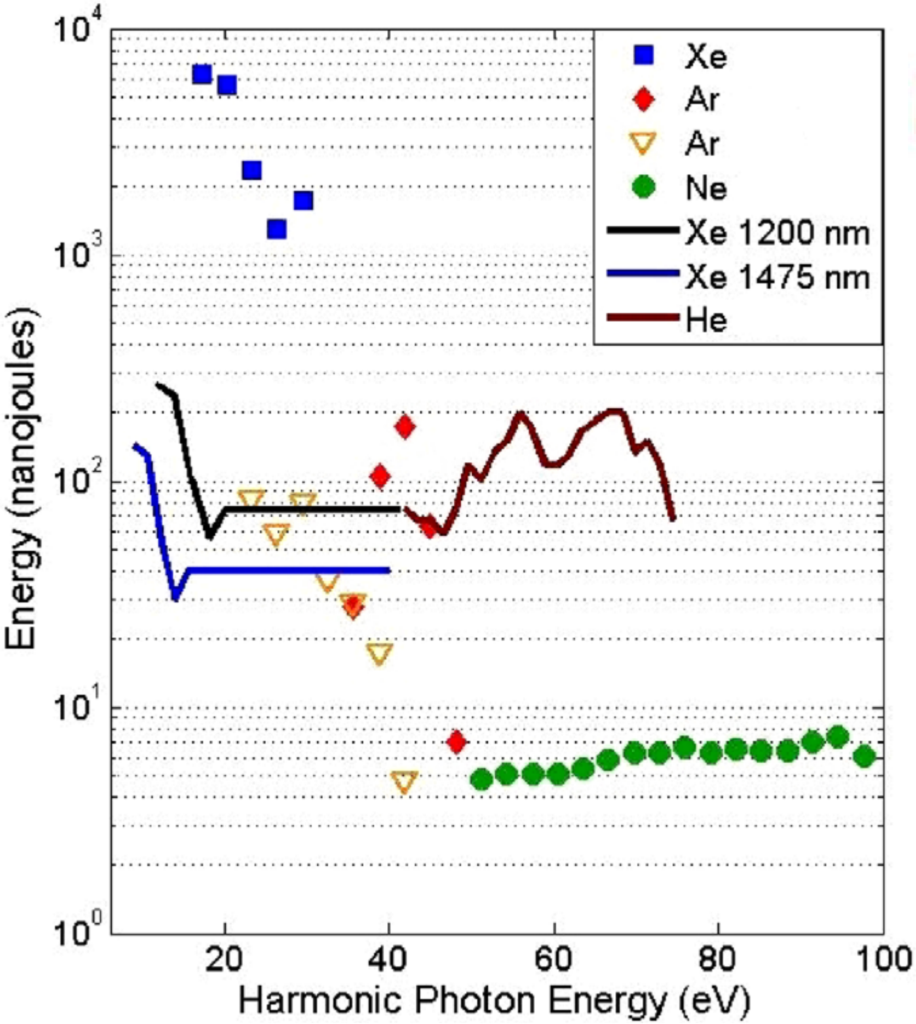

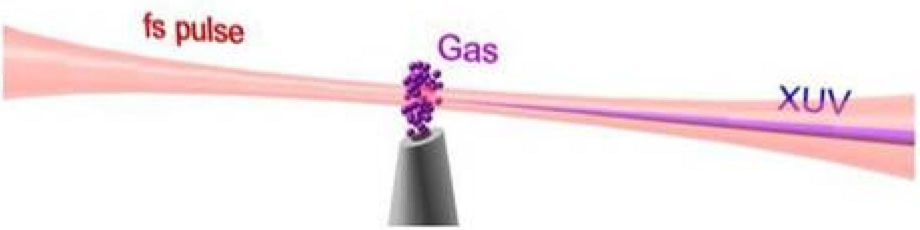

These sources result from the high harmonic emission from a gas jet of noble gas driven by a high power laser:

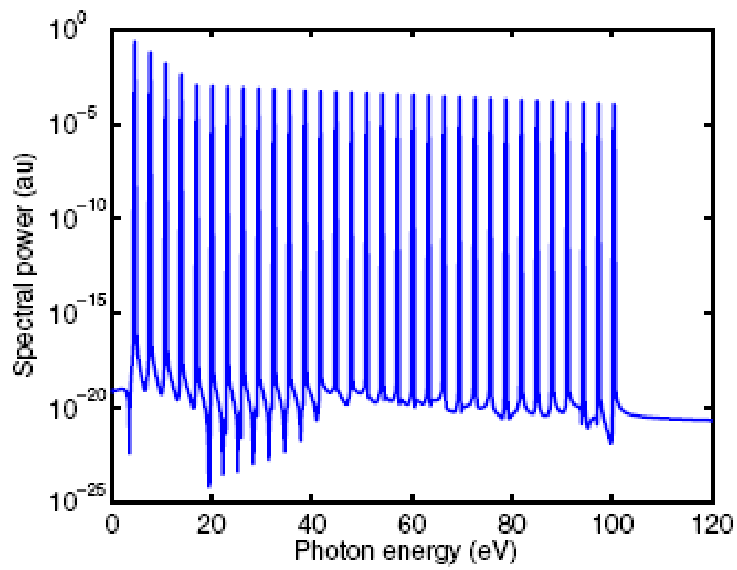

The Undulators

The resonant photon energy (eV)

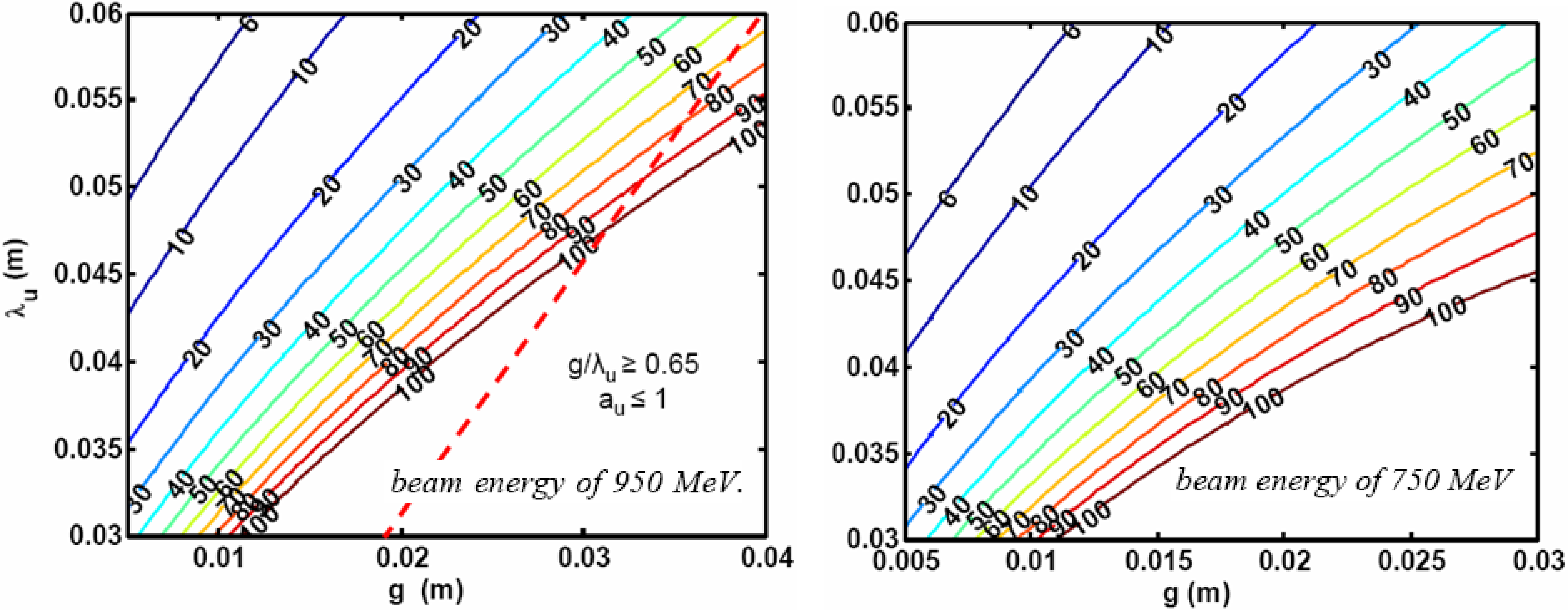

Tuning the FEL is achieved by varying the undulator gap and by changing the electron beam energy between 750-950MeV. For the planar undulators above a period of 45mm was chosen to enable tuning over the photon energy range 10-100eV.

Undulator lattice

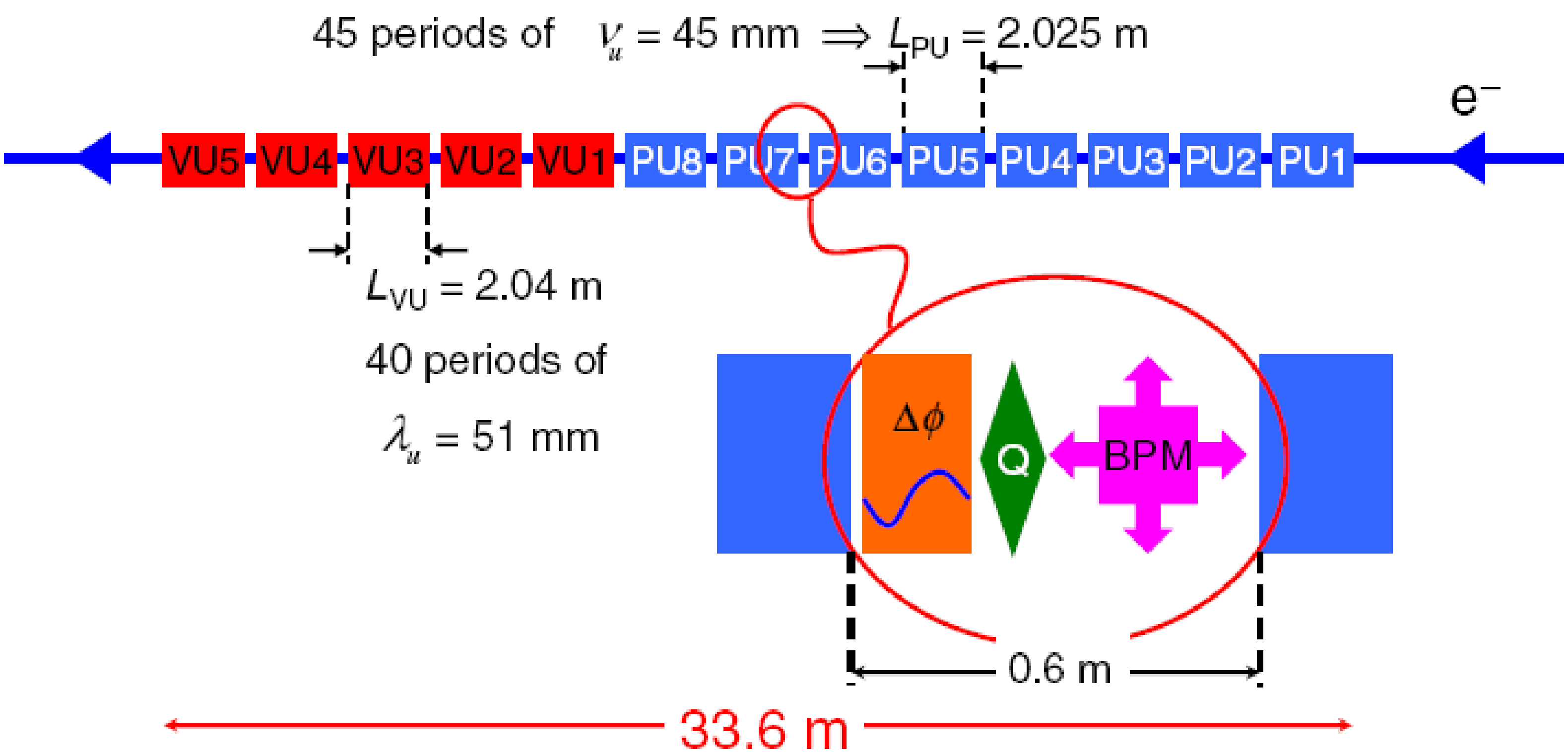

The undulator is split into many modules of length ~2m each (PU - planar undulator; VU - variable polarisation undulator). Between each module are phase-matching magnets, quadrupole focussing units for electron transport (a FODO lattice is used) and beam positioning monitors. Note the use of the variable polarisation units in the last few undulator sections to give variably polarised radiation output.

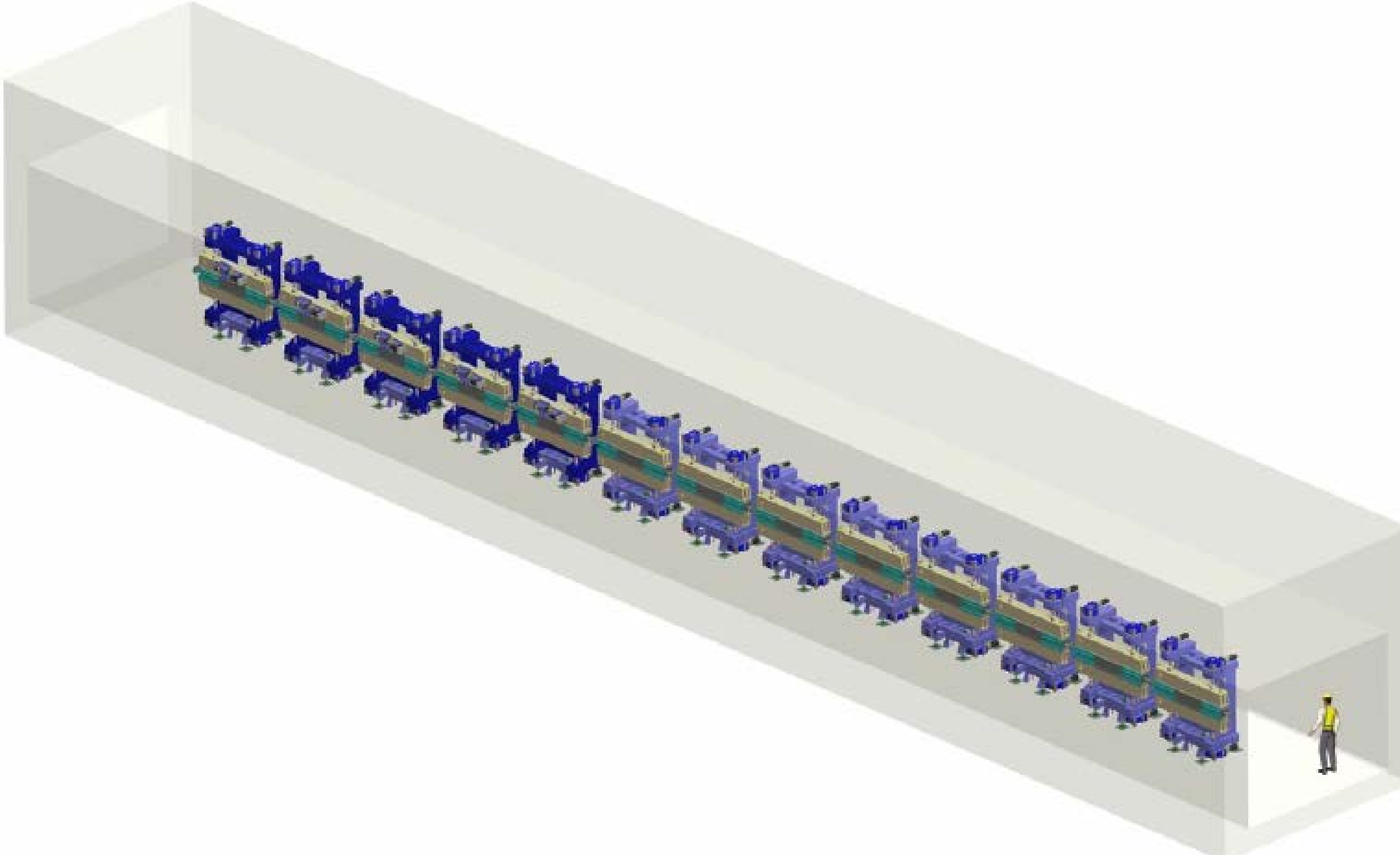

Figure 8.5 An engineering design drawing of the XUV-FEL undulator tunnel. The electron beam direction is right to left. The first eight undulator modules are planar and the last five are APPLE-II.

Figure 8.7 Schematic of the modular undulator system of the XUV-FEL demonstrating the different modes of operation across the photon energy range 10-100 eV. Undulator modules marked in grey have large magnetic gaps $\left(\lim \overline{a}_u \rightarrow 0\right)$ *and do not affect FEL operation. Electron beam transport is right to left. The minimum required undulator gap (and vacuum vessel internal aperture) decrease in gradual steps from 28 mm (25 mm) for PU1 down to 10 mm (7 mm) for PU8 and the variable polarisation modules VU1-VU5.*

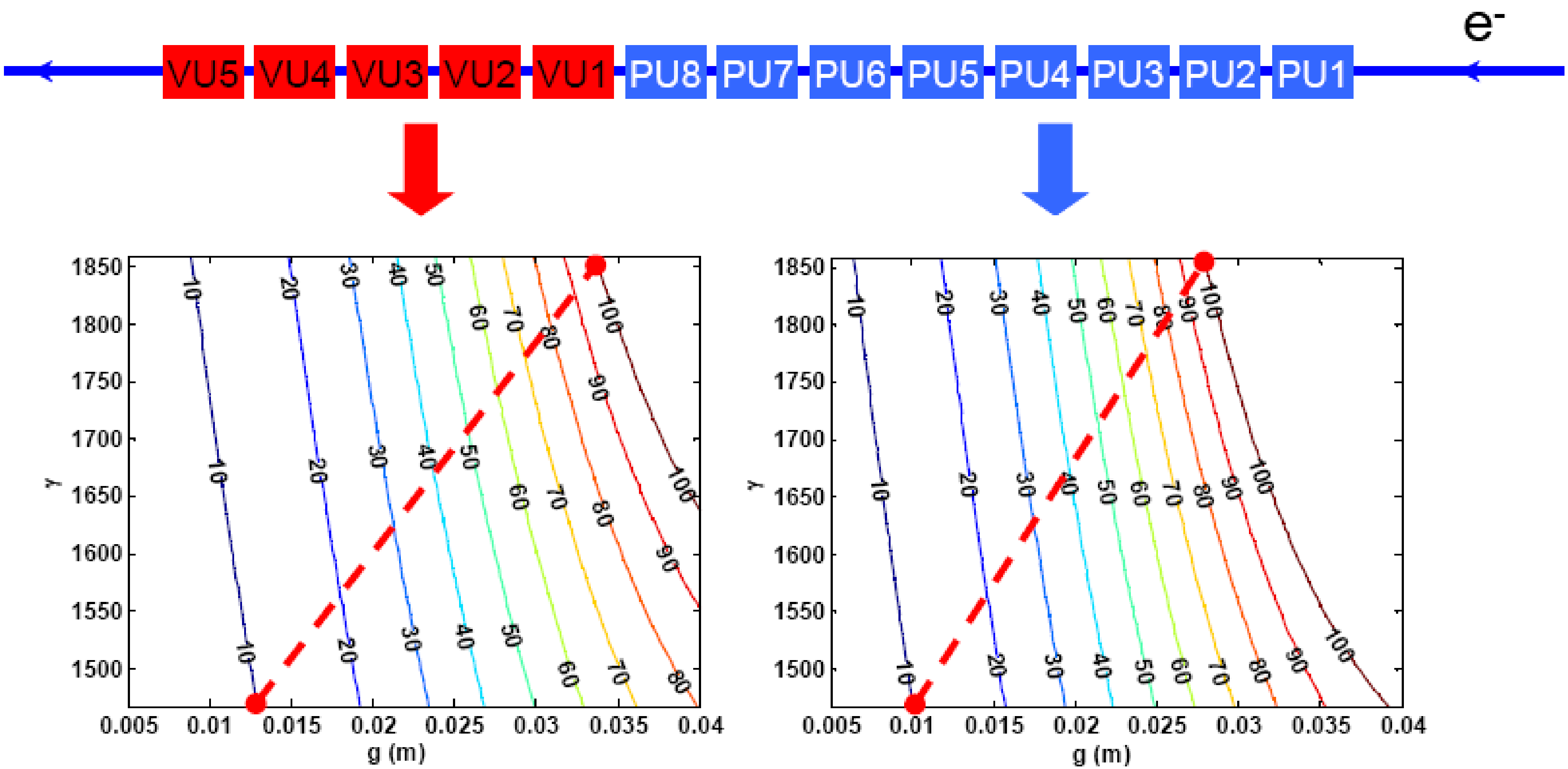

Figure 8.12 Tuning contours of the resonant photon energy (10 - 100 eV) as a function of the electron beam relativistic parameter (E_0 = 750 - 950 MeV) and the undulator magnetic gap g. The variable polarisation undulators VU1..5 are set to planar mode so that output radiation is linearly polarised. The red annotation shows the range only, not necessarily the optimum tuning curve.

Optimising the focussing lattice

Gain length

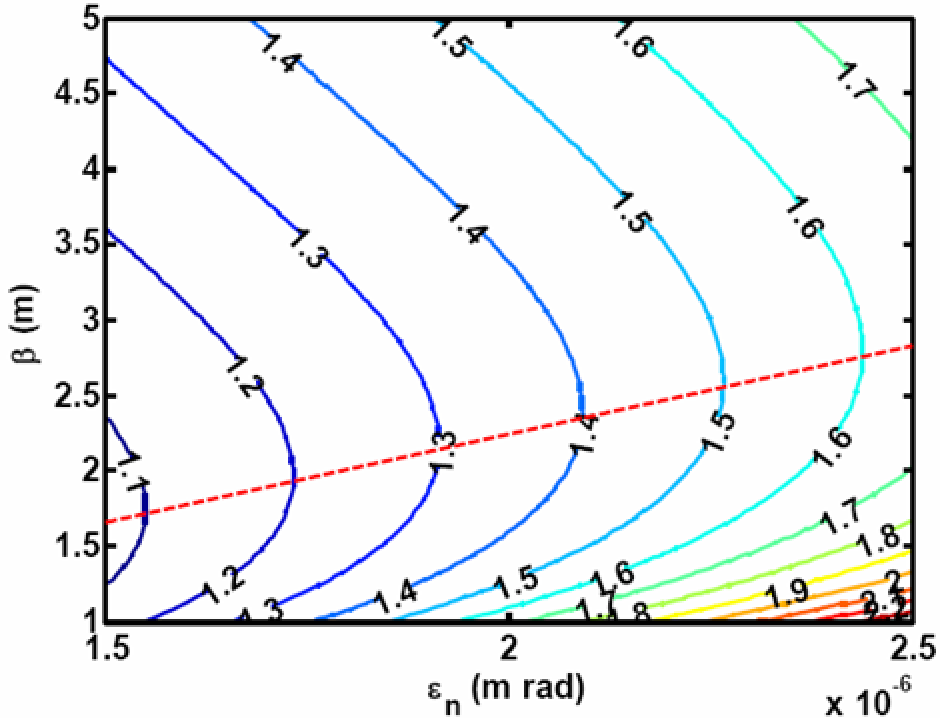

Saturation power

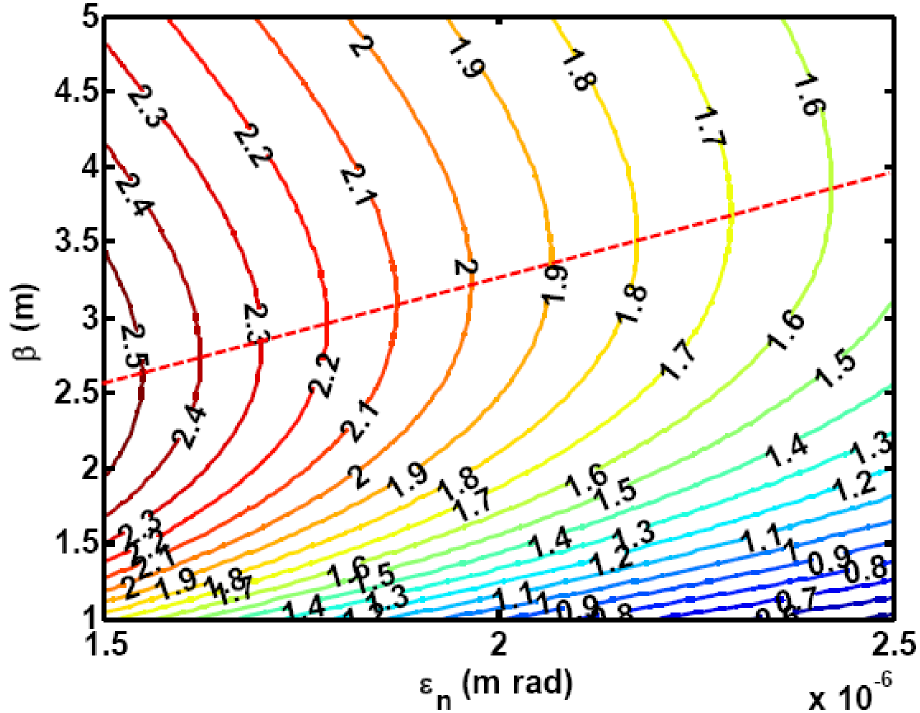

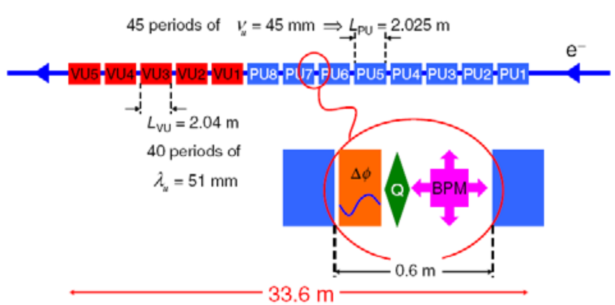

The beta-function was chosen to be ~5m. This was to stop ‘sausaging’ of the electron beam due to the variation in the beta-function of a FODO lattice:

$$\beta = \frac{2\gamma m_e c}{e L_Q B_Q} \pm \frac{\lambda_{FODO}}{2} \quad \Rightarrow \quad r_b = \sqrt{\frac{\varepsilon_n \beta}{\gamma}} \quad \text{oscillates.}$$

Beam quality

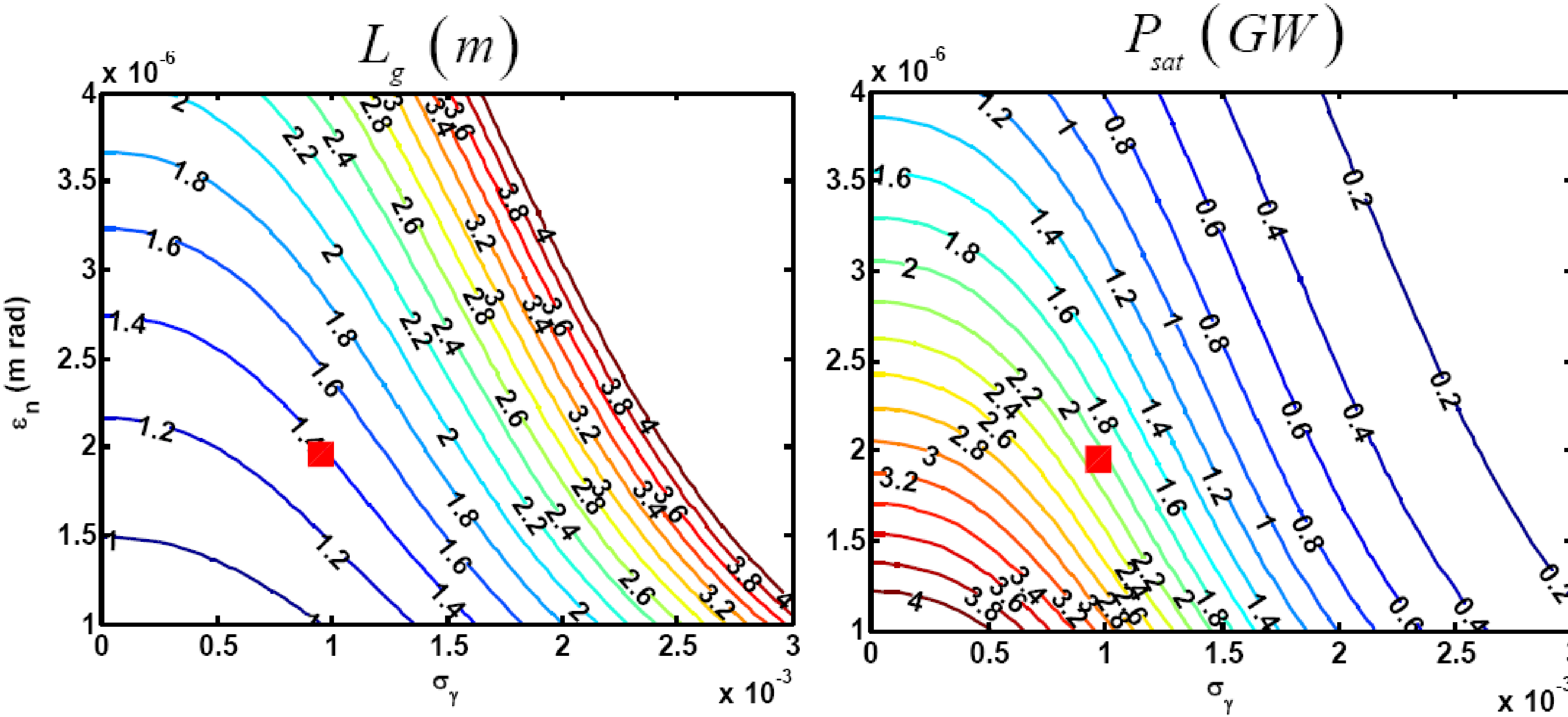

The gain length and the saturated power for 100eV operation

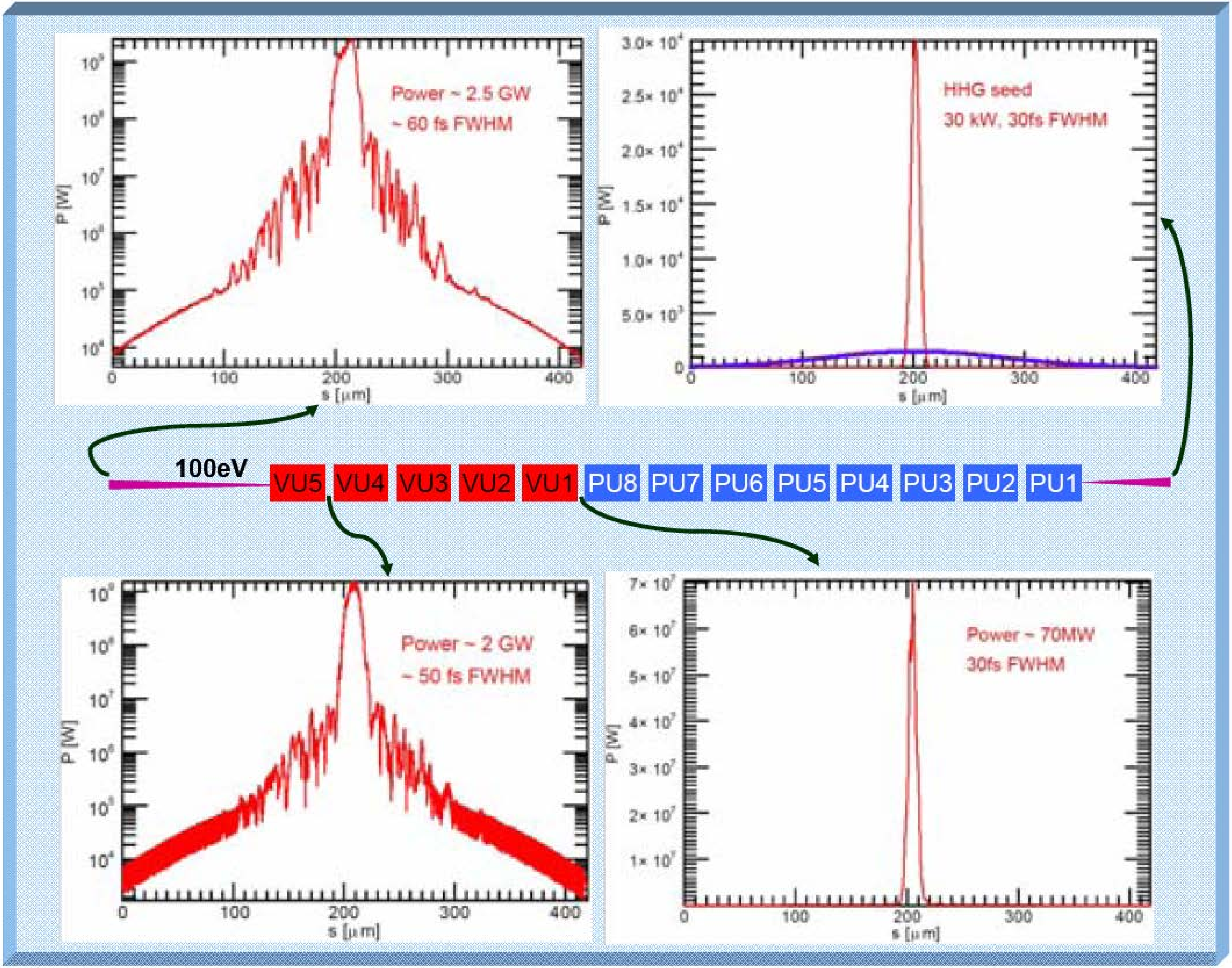

Power ~ 2.5 GW
~ 60 fs FWHM
HHG seed
30 kW, 30fs FWHM
100eV
VU5
VU4
VU3
VU2
VU1
PU8
PU7
PU6
PU5
PU4
PU3
PU2
PU1
Power ~ 2 GW
~ 50 fs FWHM
Power ~ 70MW
30fs FWHM
P [W]
s [μm]

VUV-FEL 3-10eV

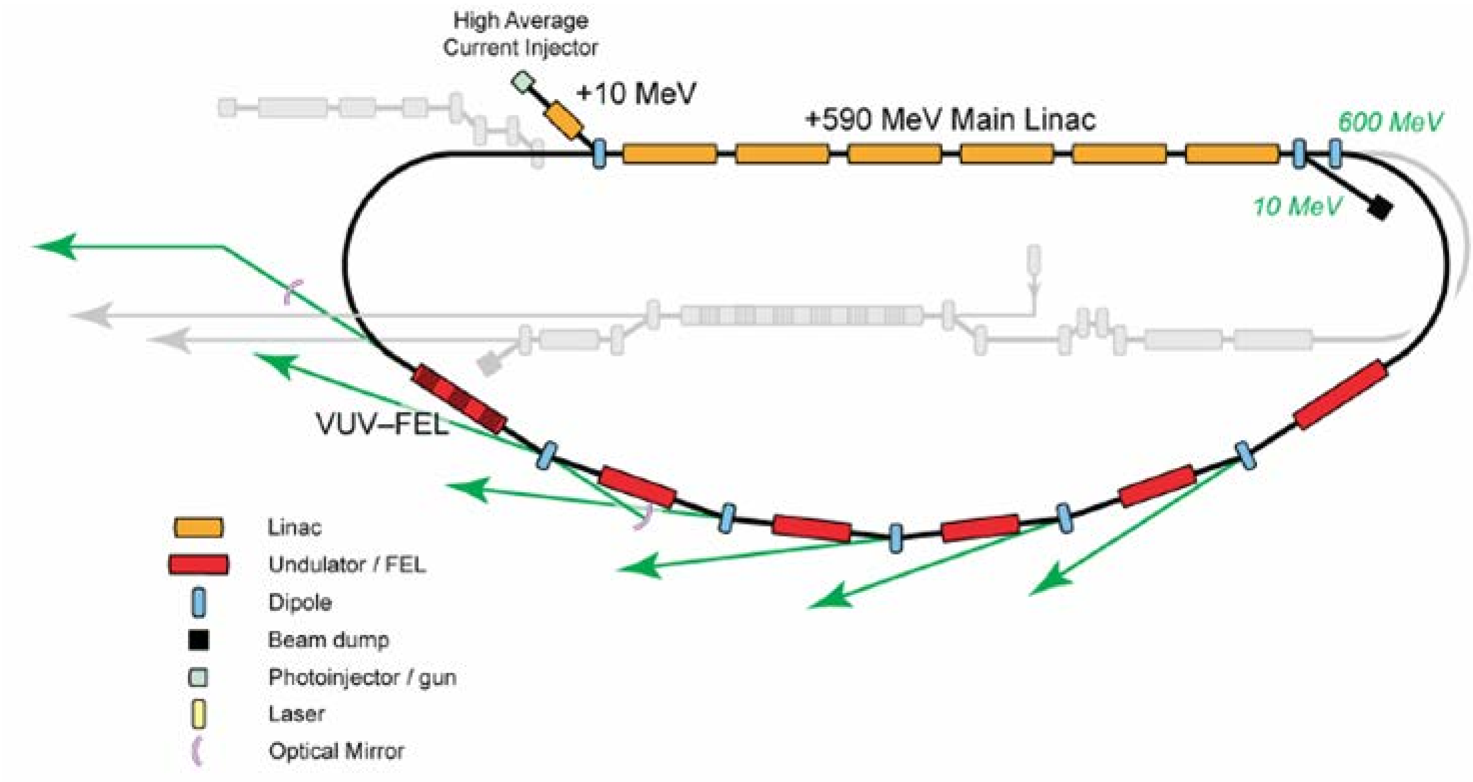

Figure 8.49 Schematic showing the main components relevant to the VUV-FEL

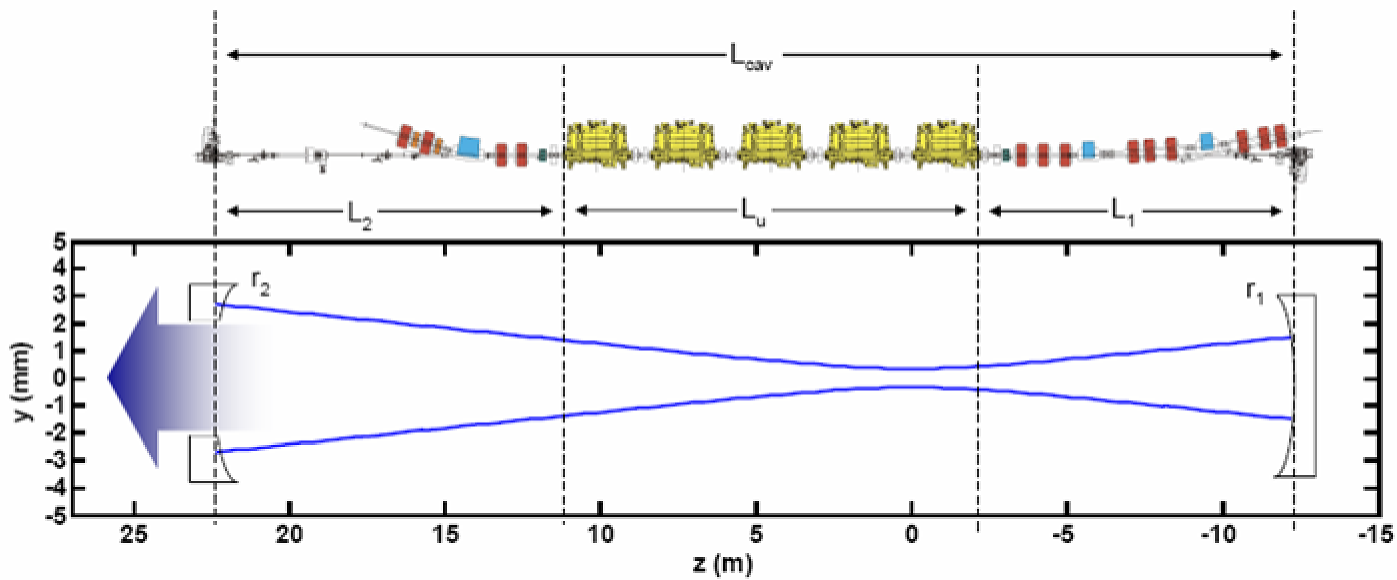

Figure 8.53 Schematic of the first iteration of the VUV-FEL low-Q cavity. Shown aligned on the same longitudinal scale is an engineering representation of the VUV-FEL. The radius of curvature, r_2, of the hole-outcoupling mirror is greater than that of the upstream mirror, r_1. This cavity design has a minimum beam waist nearer the entrance to the undulator assisting the self-seeding process.

	Planar			***Helical***		
	L_g	ρ	$\overline{Z}$	L_g	ρ	$\overline{Z}$
10 eV	1.81 m	1.52×10^{-3}	3.52	1.24 m	2.22×10^{-3}	5.16 (5 mods)
						4.13 (4 mods)
3 eV	1.38 m	2.00×10^{-3}	4.64 (5 mods)	0.87 m	3.17×10^{-3}	7.38 (5 mods)
			3.71 (4 mods)			5.90 (4 mods)
						4.43 (3 mods)

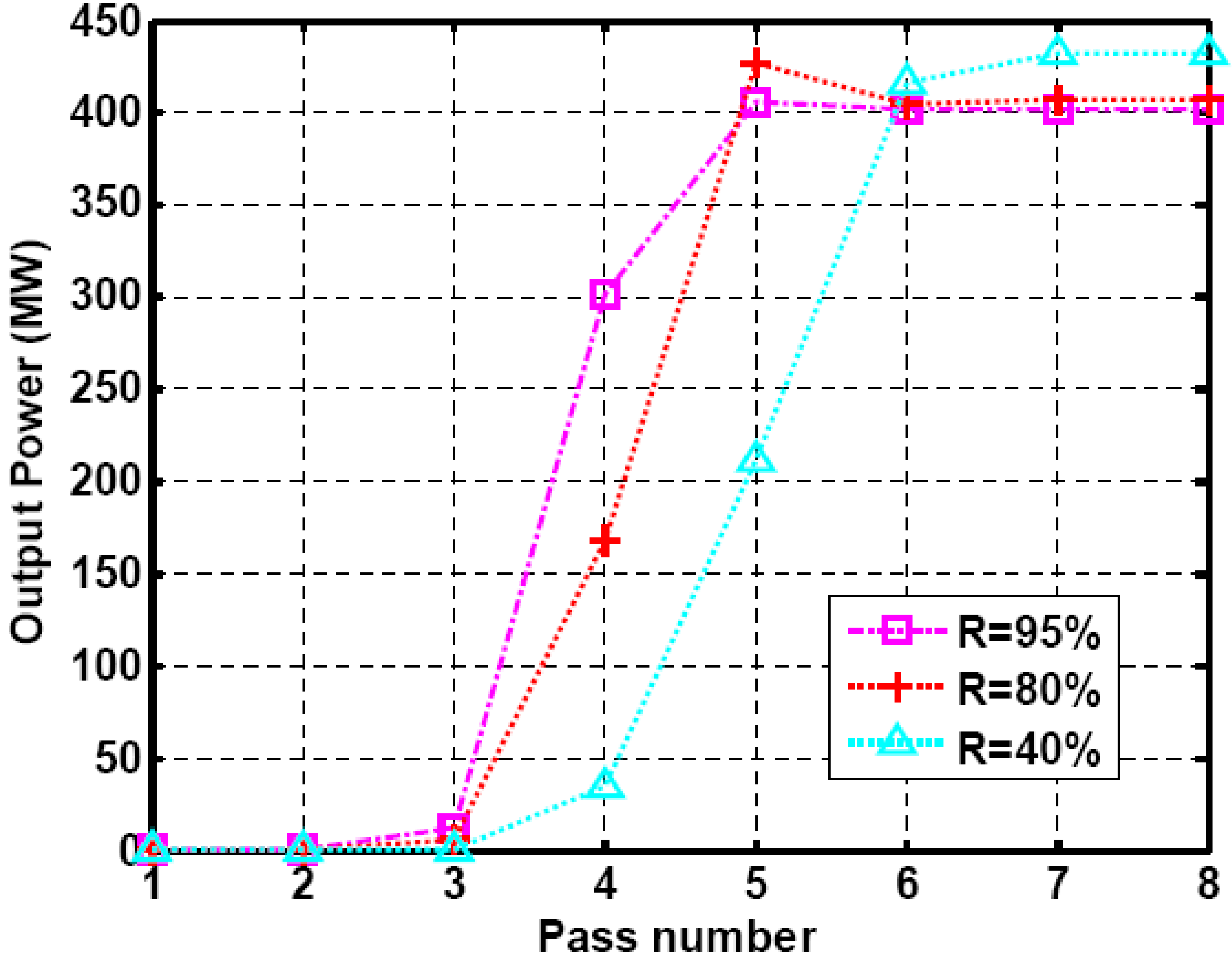

Figure 8.55 Three-dimensional steady-state simulation of the VUV-FEL operating at 10 eV photon energy. The output power is plotted as a function of optical pass number through the cavity for an outcoupling factor of α = 75% and for three different mirror reflectivities.

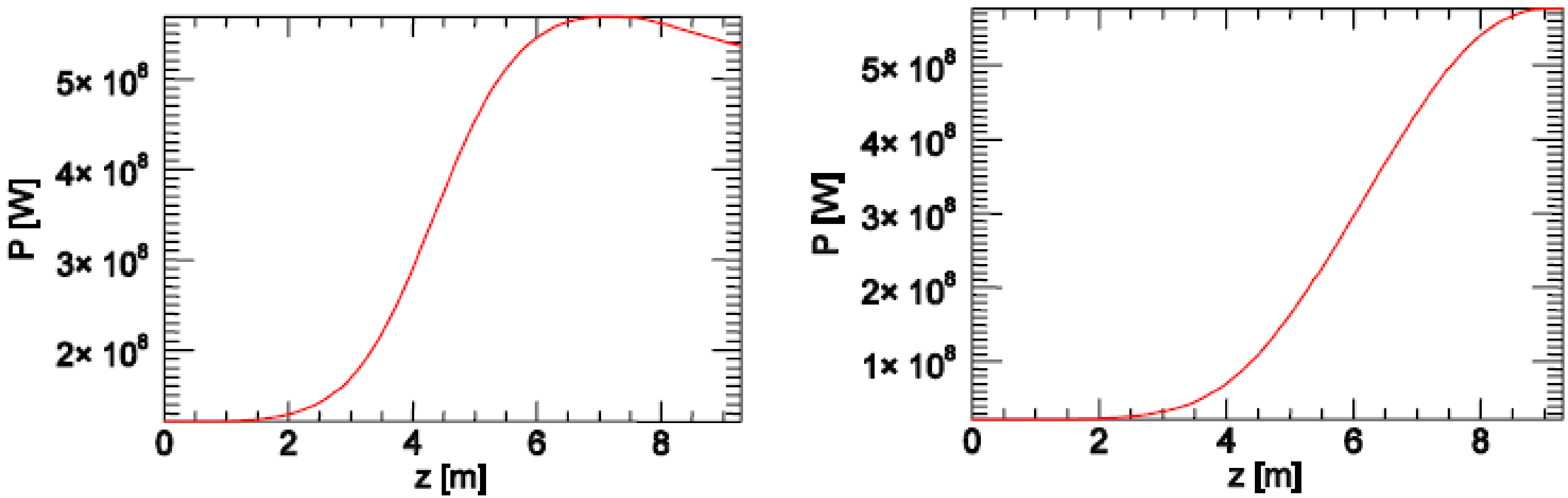

Figure 8.56 Power evolution of the radiation through the undulator at cavity saturation for the case of 95 % mirror reflectivity (left) and 40 % reflectivity (right). For 95 % reflectivity the FEL power oversaturates, whereas for 40 % reflectivity the power saturates exactly at the end of the undulator, leading to optimum outcoupled power.

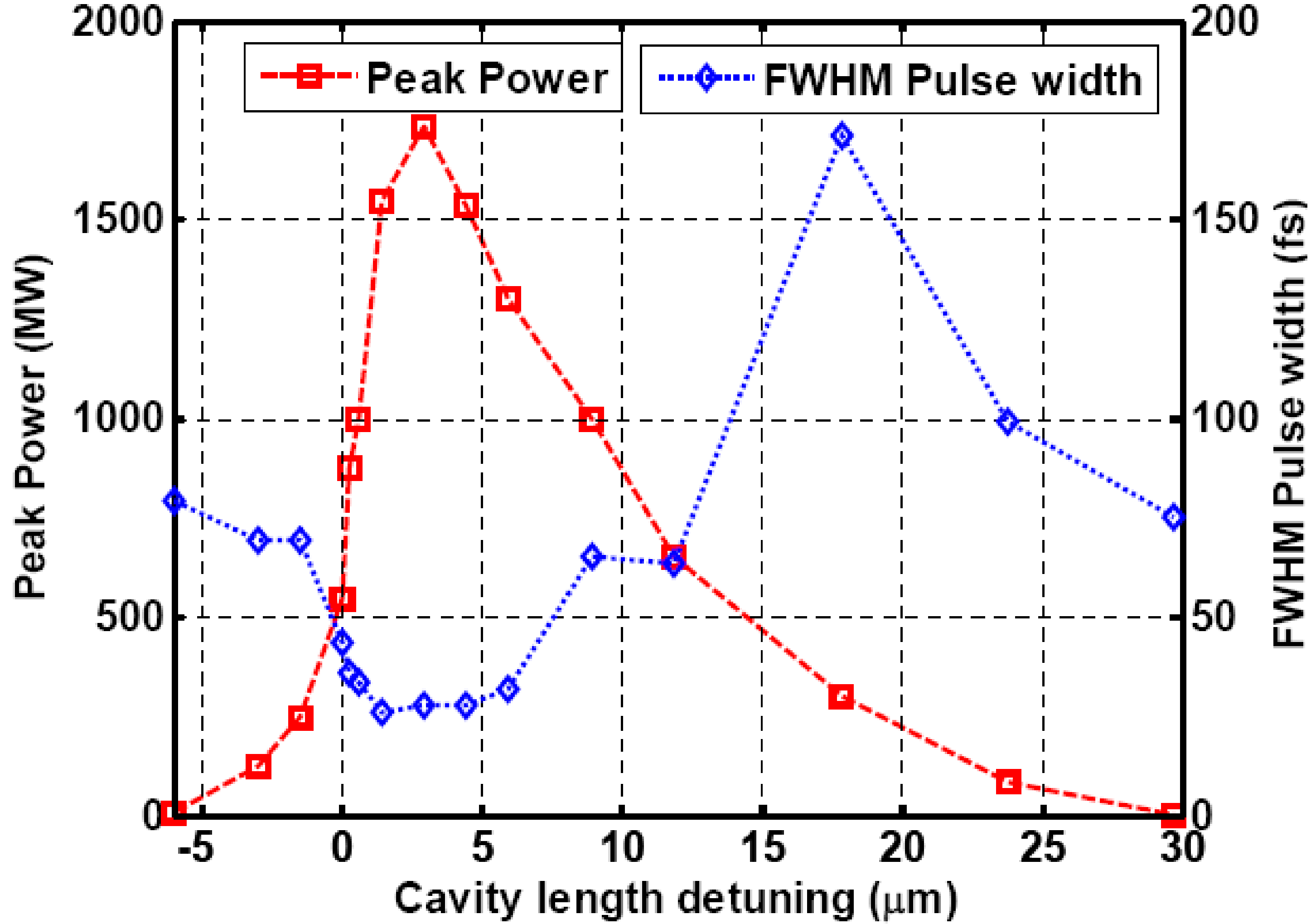

Figure 8.57 Peak power (red) and FWHM pulse width (blue) as a function of VUV-FEL cavity detuning. The parameters are for 10 eV photon output.

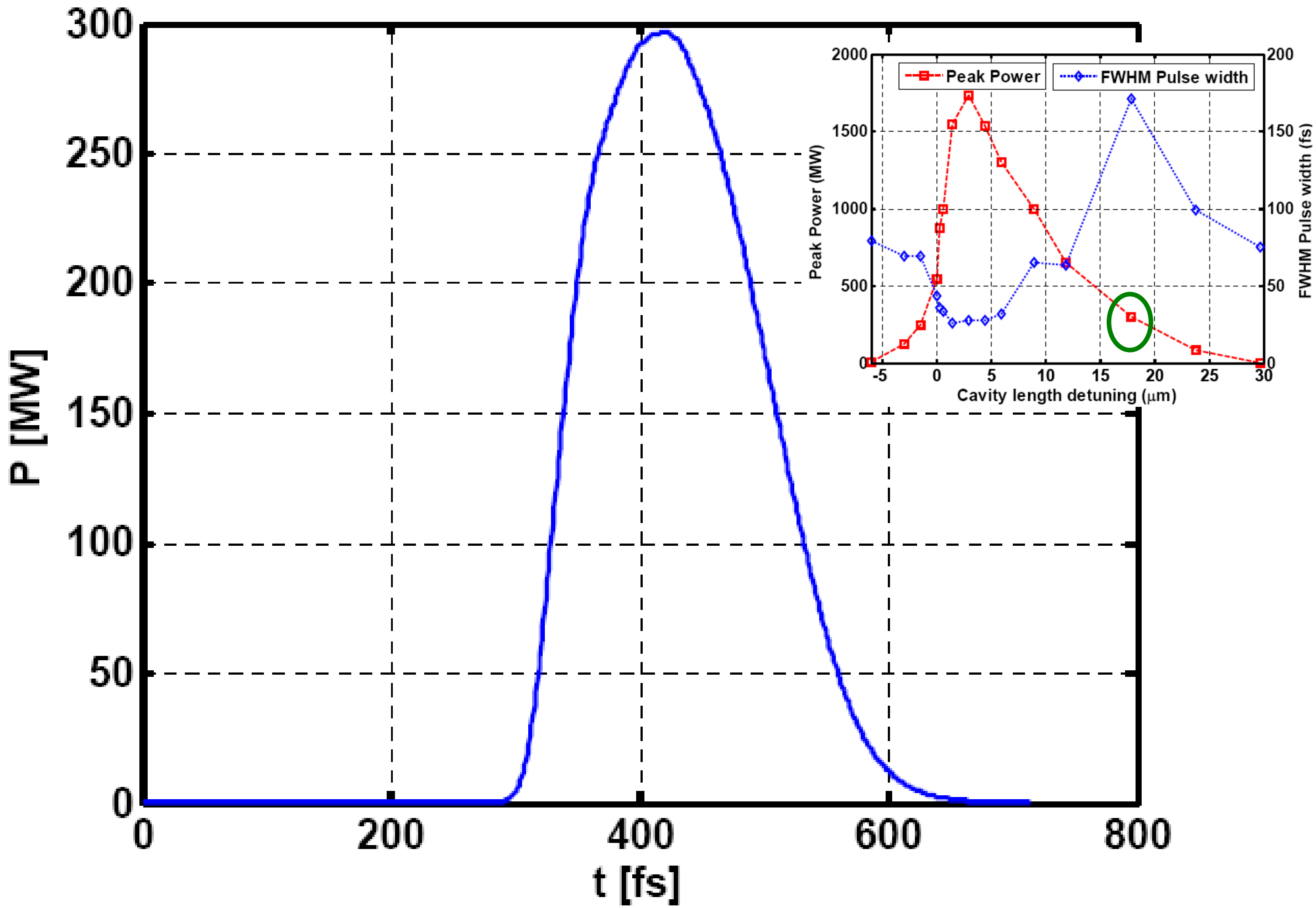

Figure 8.59 One-dimensional simulation result showing the 10 eV radiation power at saturation as a function of time for cavity detuning $\delta_c \approx 18\,\mu\mathrm{m}$. *The pulse shape demonstrates none of the superradiant behaviour of Figure 8.58*

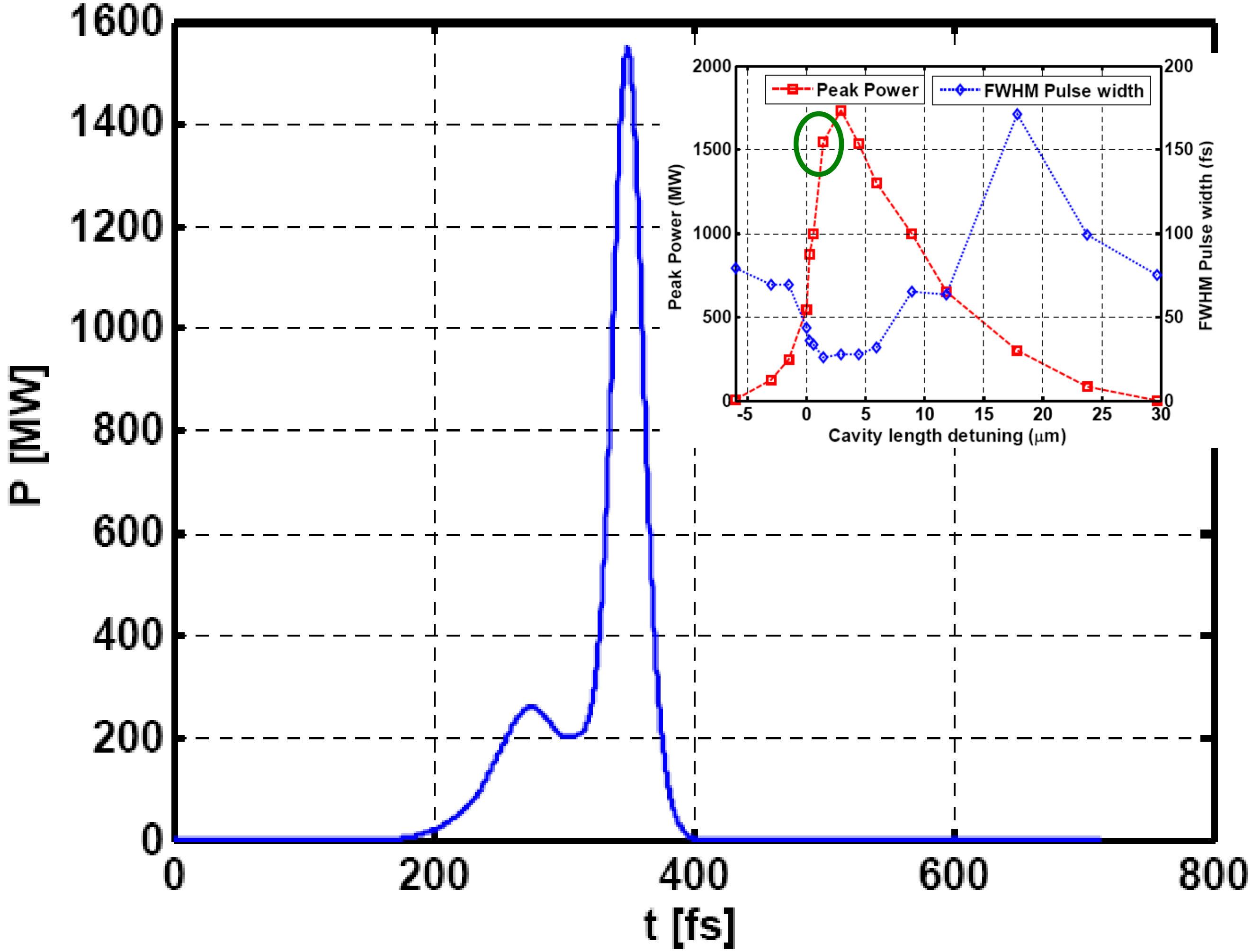

Figure 8.58 One-dimensional simulation result showing the 10 eV radiation power at saturation as a function of time for near- zero cavity detuning. The pulse shape demonstrates a spiking behaviour typical to FEL superradiance.

IR-FEL 2.5-200μm

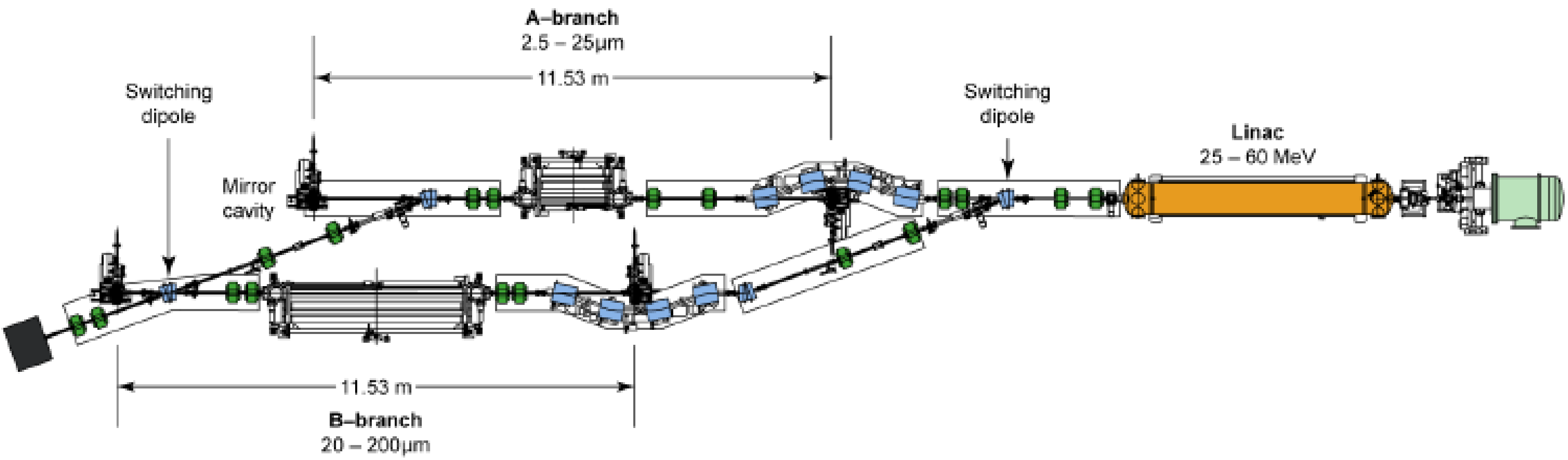

Figure 8.64 Conceptual layout of the IR-FEL showing the two undulator branches

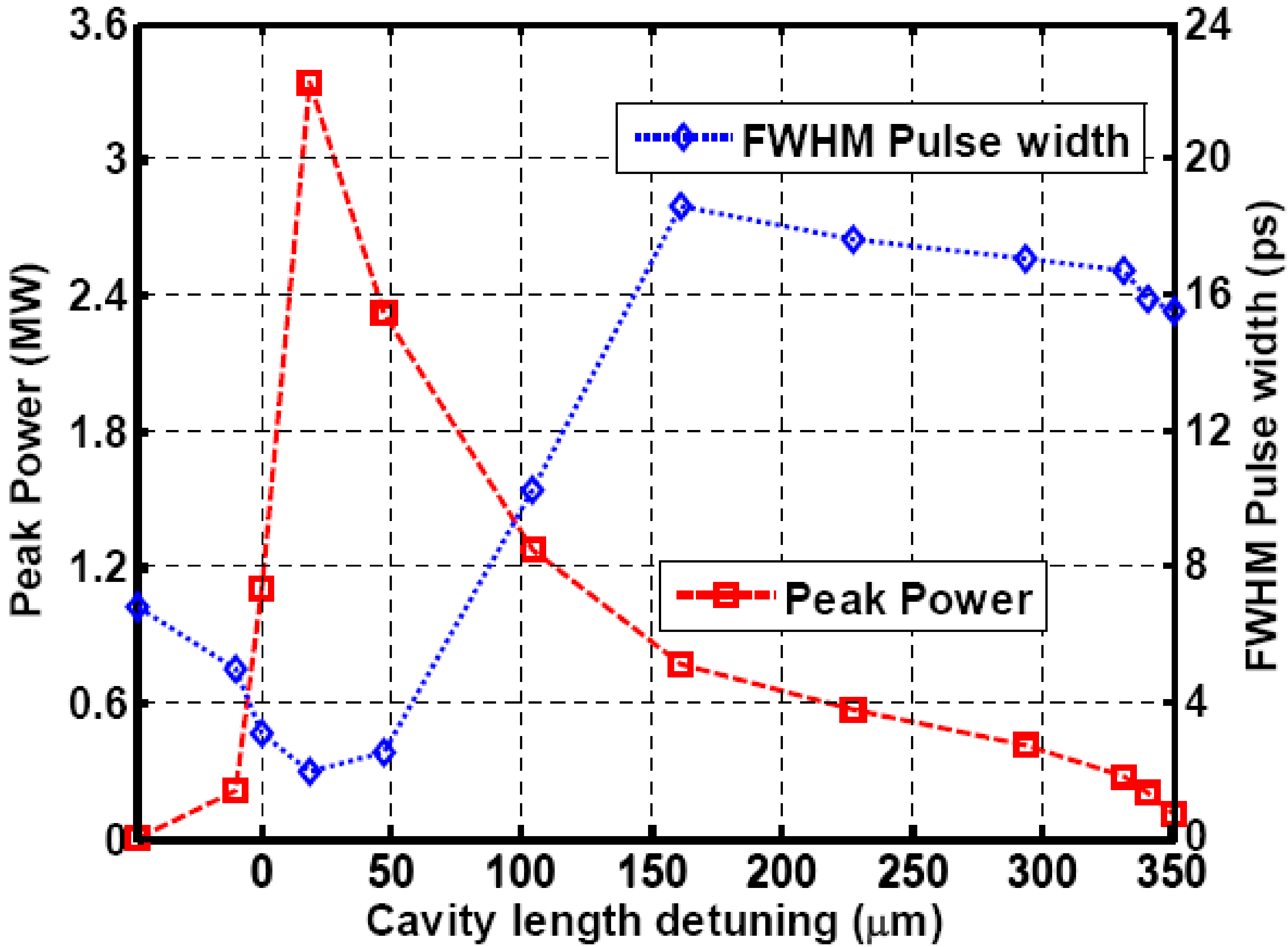

Figure 8.75 Peak power and FWHM pulse width as a function of cavity length detuning, for IR-FEL A-Branch at 25 μm with 10 ps electron bunches

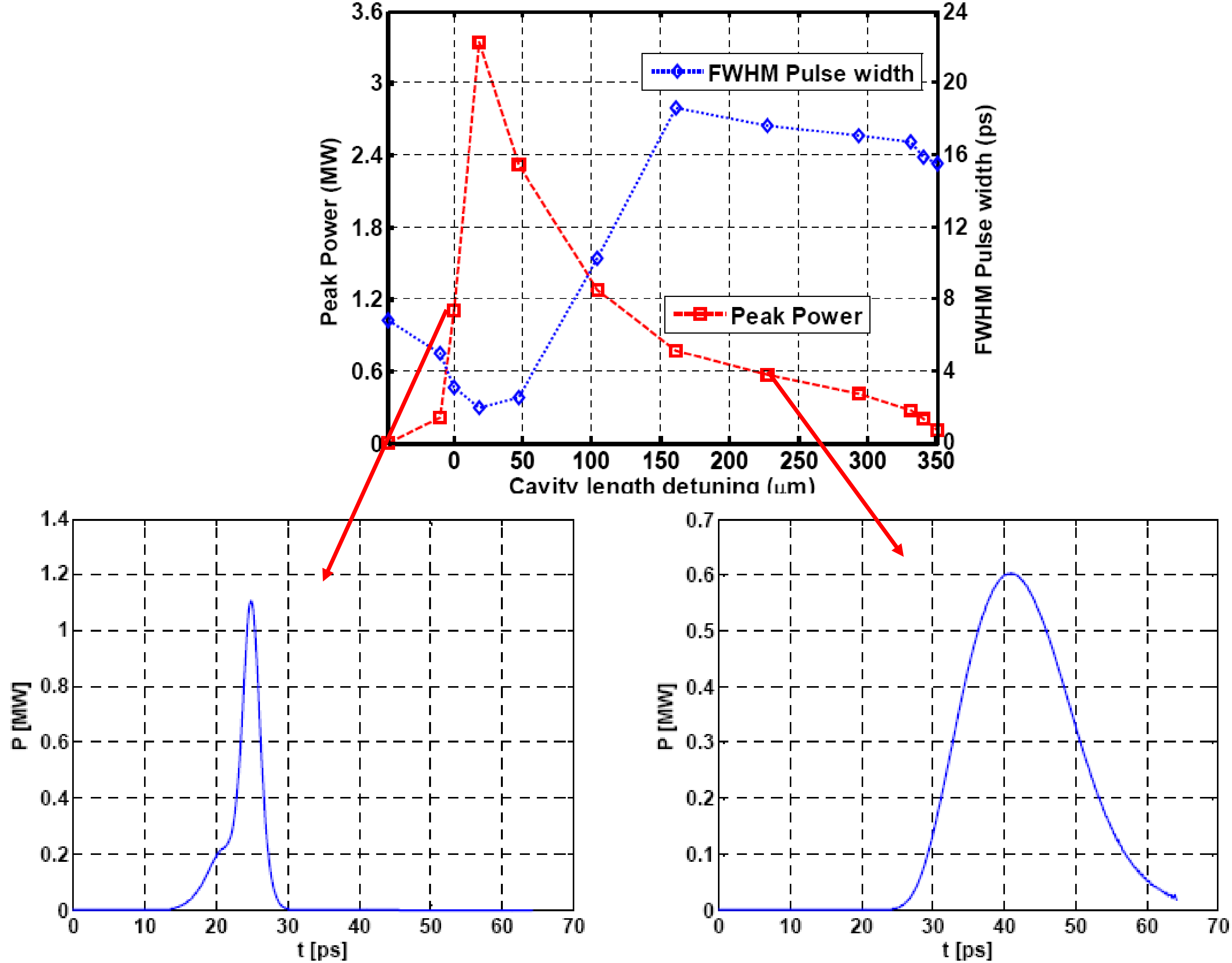

Figure 8.76 IR-FEL A-Branch 25 µm pulse profile corresponding to a synchronous cavity length (left) and detuned by 227 µm (right)

DESCRIPTION	
FEL design	Oscillator
Seeding type	Self-seeding
Seeding mechanism	High-Q cavity
PHOTON OUTPUT	
Tuning Range	2.5 - 200 μm
Peak Power	9 MW (>20 MW) - 1 MW (>4 MW*)
Pulse length FWHM	2 ps (300 fs*) - 10 ps (6 ps*)
Repetition rate	13 MHz
Polarisation	Variable elliptical
Typical $\Delta\nu\Delta t$	≈ 0.9
Max pulse energy	≈ 50 μJ
ELECTRON BEAM PARAMETERS	
Energy	25 - 60 MeV
Bunch Charge	200 pC
RMS bunch length	1 - 10 ps
Normalised emittance	10 mm mrad
RMS energy spread	0.1 %
UNDULATOR PARAMETERS	
Undulator Type	APPLE-II
No of Modules	1 /1
Module length	2.65 m / 5.07 m
Period	53 mm / 145 mm
Focussing	Natural
Minimum gap	23.5 mm / 74 mm
OPTICAL CAVITY PARAMETERS	
Length	11.53 m
Rayleigh length	0.94 m / 2.05 m
Stability parameter g^2	0.90 / 0.60
Mirror diameter	100 mm / 180 mm

* indicates possible output in superradiant mode

Some advanced schemes

2-undulator concept

An electron beam bunched at a fundmental wavelength also has a stron bunching component at harmonics of the fundamental.

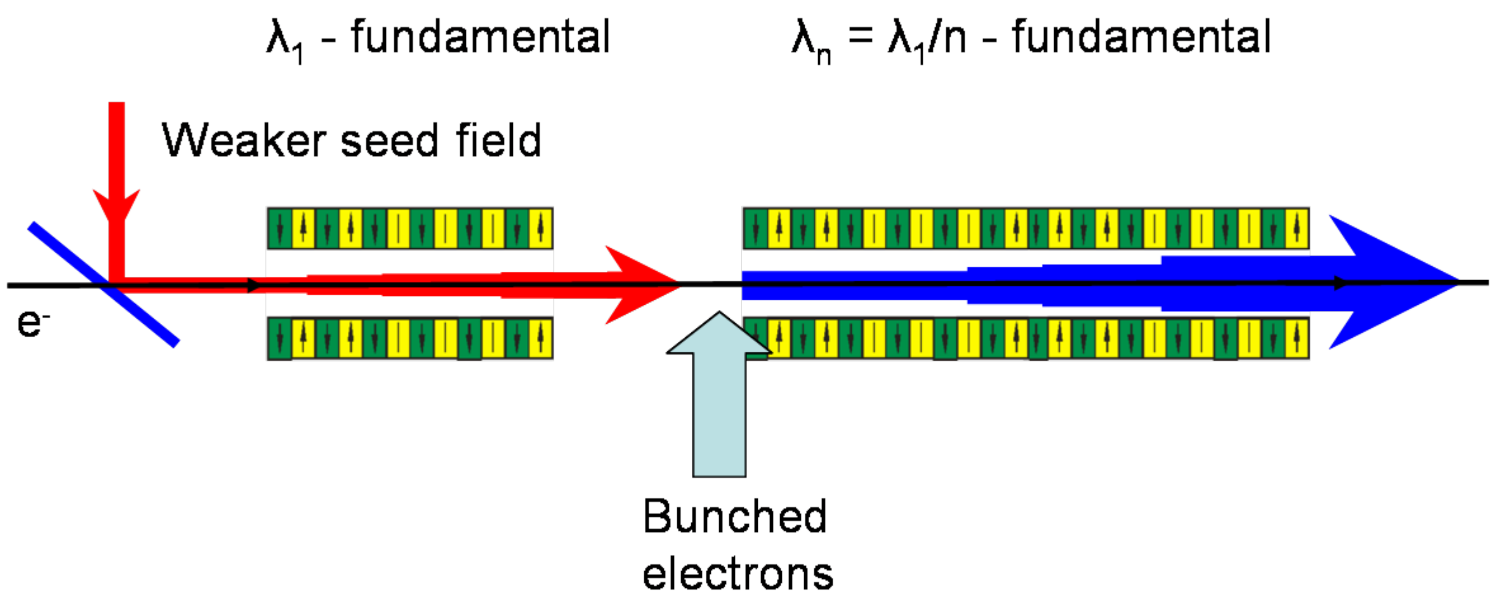

R. Bonifacio, L. De Salvo Souza, P. Pierini, and E. T. Scharlemann, Nucl. Instrum. Methods A **296**, 787 (1990).

R. Bonifacio, R. Corsini, and P. Pierini, Phys. Rev. A **45**, 4091 (1992).

HGHG concept

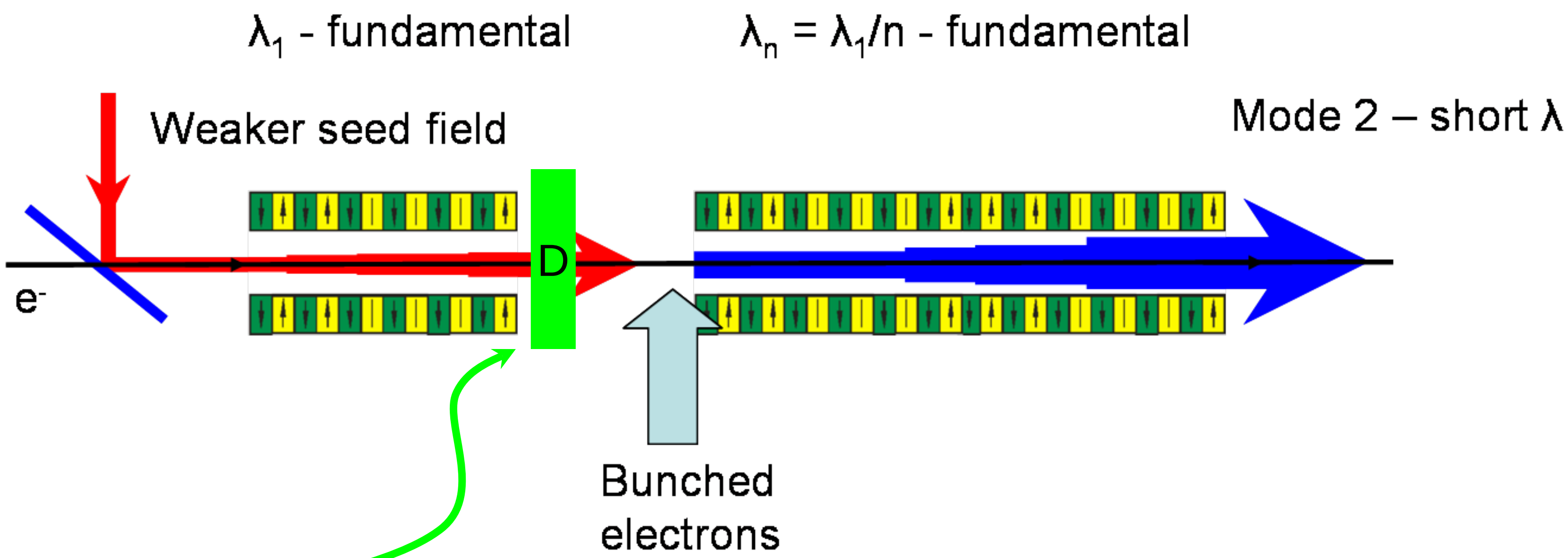

$$D = k\rho R_{56}$$

L. H. Yu, Phys. Rev. A **44**, 5178 (1991)

2-beam FEL amplifier

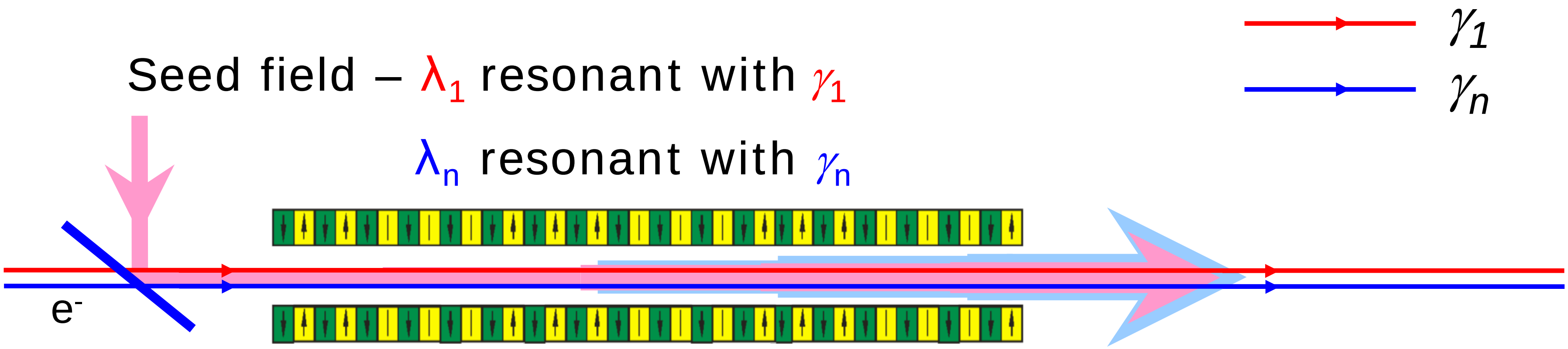

By choosing $\gamma_n = \sqrt{n}\,\gamma_1$ the fundamental resonant wavelength of beam γ_n is the n^{th} resonant harmonic of beam γ_1.

The coherence properties of the seed field will be transferred to the higher energy interaction via the coupled harmonic interaction.

B. W. J. McNeil* and G. R. M. Robb PHYSICAL REVIEW E **70**, 035501(R) (2004)

A compact synchrotron radiation source driven by a laser-plasma wakefield accelerator

H.-P. SCHLENVOIGT[1], K. HAUPT[1], A. DEBUS[1], F. BUDDE[1], O. JÄCKEL[1], S. PFOTENHAUER[1], H. SCHWOERER[1,2], E. ROHWER[2], J. G. GALLACHER[3], E. BRUNETTI[3], R. P. SHANKS[3], S. M. WIGGINS[3] AND D. A. JAROSZYNSKI[3]*

nature physics | ADVANCE ONLINE PUBLICATION | www.nature.com/naturephysics

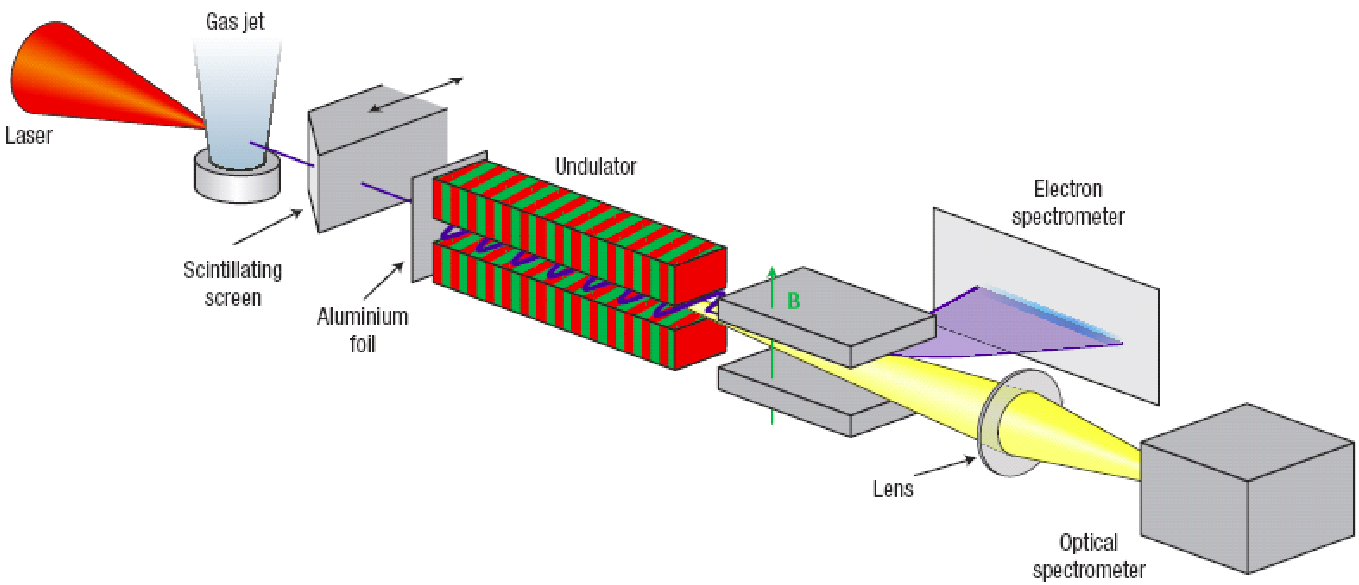

Figure 1 Set-up of the experiment. The laser pulse is focused by an off-axis parabolic mirror into a supersonic helium gas jet where it accelerates electrons (blue line) to several tens of mega-electron volt energy. The electron beam profile may be monitored by a removable scintillating screen. The electrons propagate through an undulator, producing synchrotron radiation, and into a magnetic electron spectrometer. Radiation is collected by a lens and analysed in an optical spectrometer. The spectrometer is protected against direct laser and plasma exposure by a thin aluminium foil in front of the undulator.

Harmonic Amplifier FEL

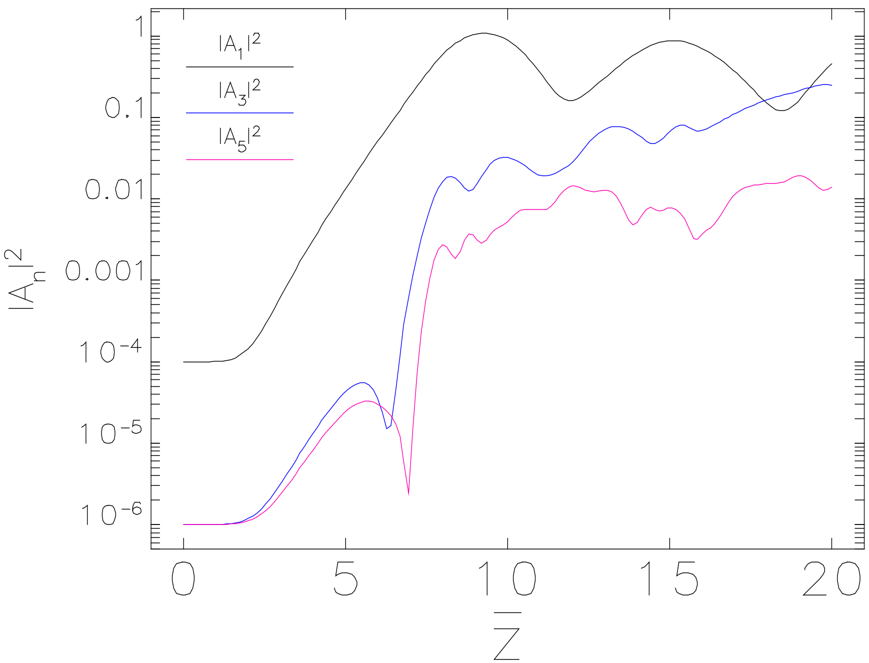

Normal planar FEL amplifier including the 3rd & 5th harmonics (Undulator a_w=3)

Harmonic Amplifier FEL demonstrating dominance of 3rd harmonic over fundamental & 5th harmonic

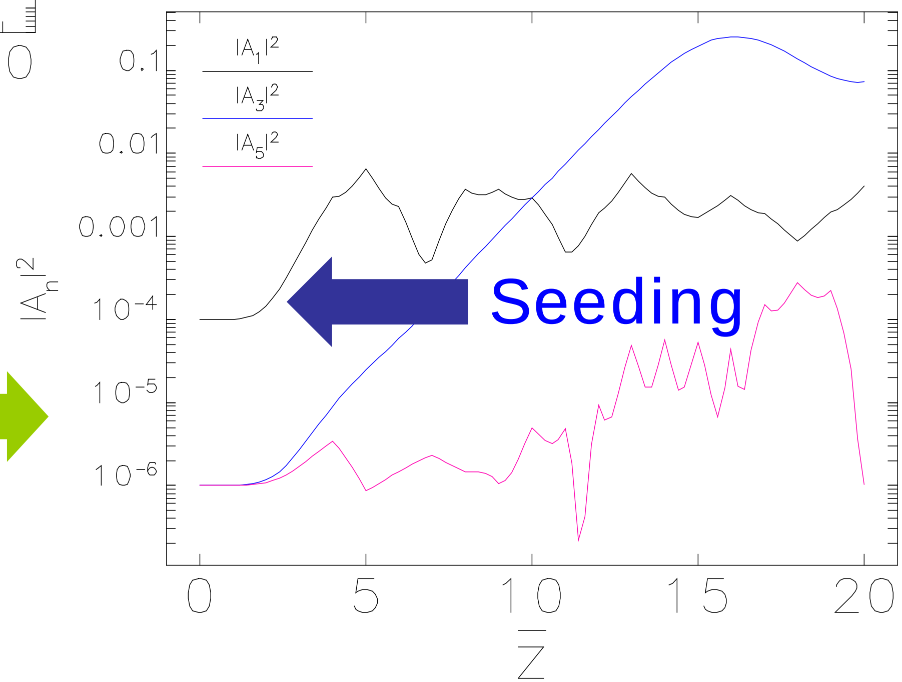

B. W. J. McNeil,[1,*] G. R. M. Robb,[1] M. W. Poole,[2] and N. R. Thompson[2] PRL **96,** 084801 (2006)

Attosecond pulse generation

VOLUME 92, NUMBER 22 PHYSICAL REVIEW LETTERS week ending 4 JUNE 2004

Proposal for Intense Attosecond Radiation from an X-Ray Free-Electron Laser

Alexander A. Zholents and William M. Fawley

PHYSICAL REVIEW SPECIAL TOPICS - ACCELERATORS AND BEAMS **8**, 040701 (2005)

Method of an enhanced self-amplified spontaneous emission for x-ray free electron lasers

Alexander A. Zholents

PHYSICAL REVIEW SPECIAL TOPICS - ACCELERATORS AND BEAMS **9**, 050702 (2006)

Self-amplified spontaneous emission FEL with energy-chirped electron beam and its application for generation of attosecond x-ray pulses

E. L. Saldin, E. A. Schneidmiller, and M. V. Yurkov

Mode-Locked SASE FEL

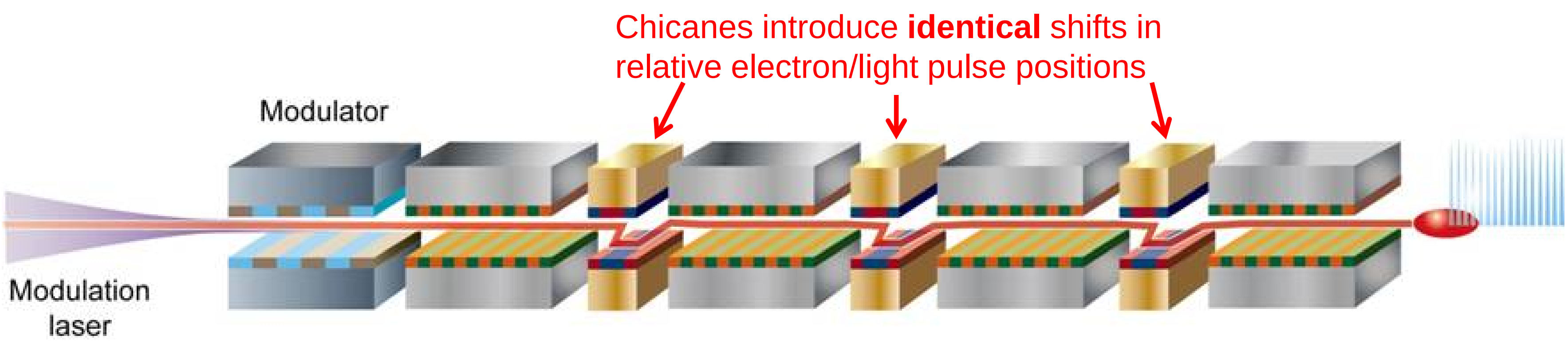

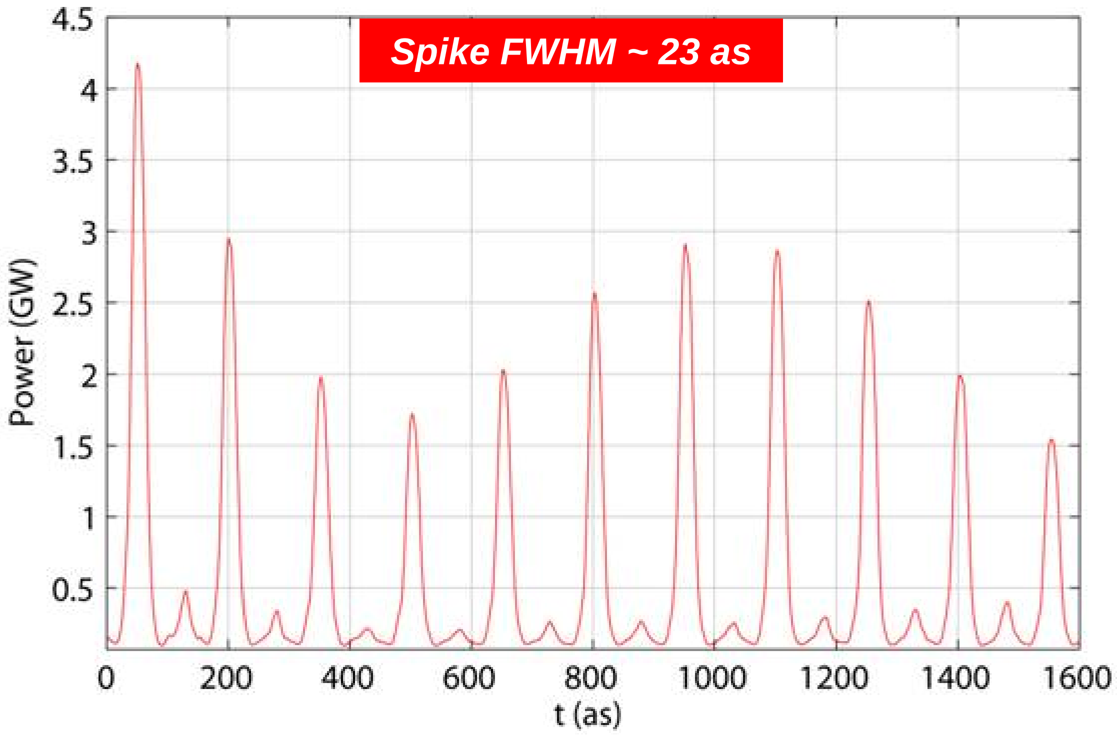

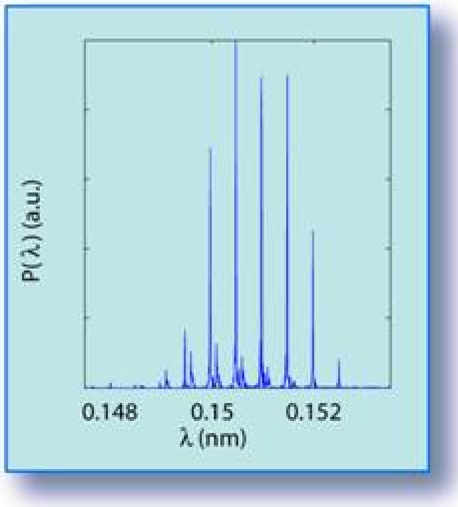

N. R. Thompson[1,2,*] and B. W. J. McNeil[1,†] PRL **100,** 203901 (2008)

Mode-Locked Afterburner*

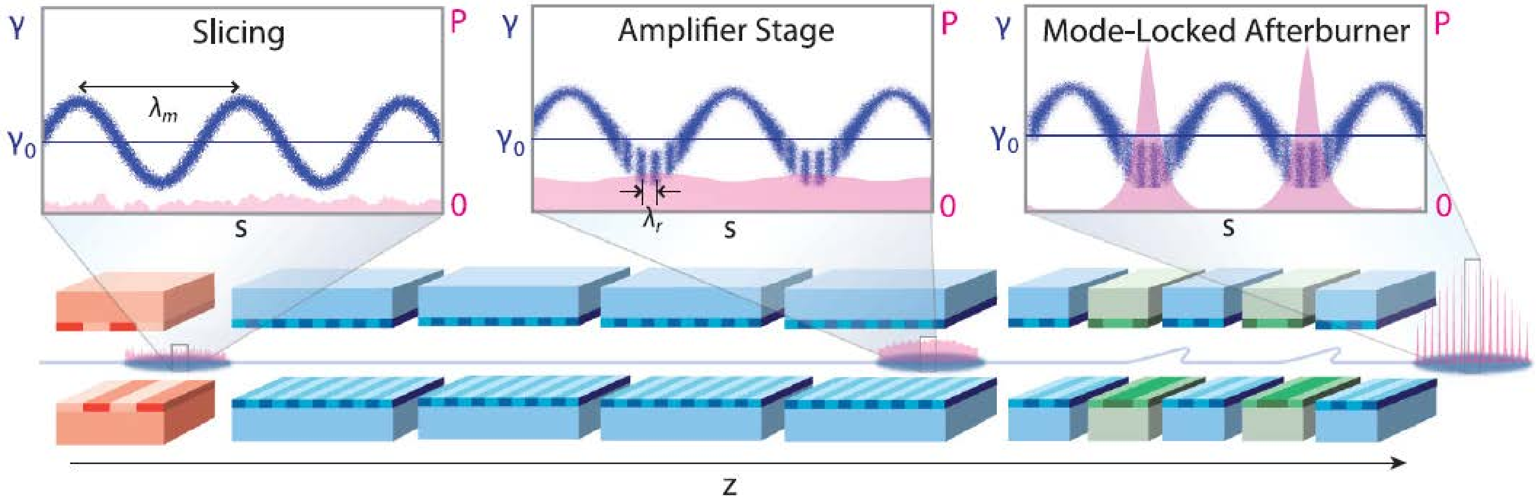

Can generate few-cycle pulses – this takes x-ray FELs into the zeptosecond regime (10^{-21}s)

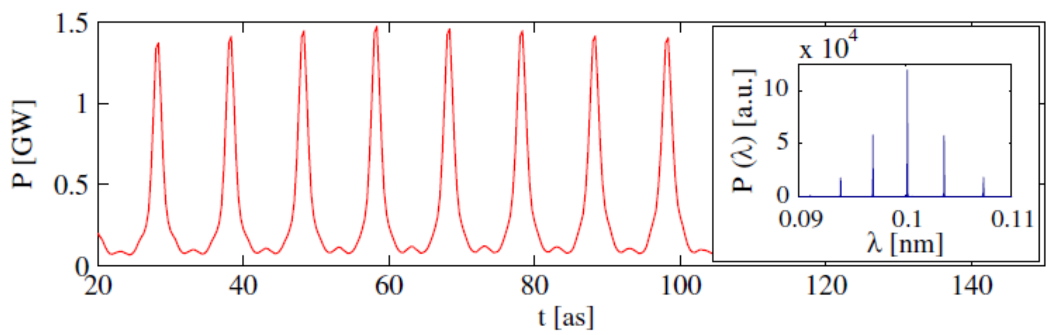

FIG. 4 (color online). Hard x-ray mode-locked afterburner simulation results: Radiation power profile and spectrum after 40 modules. The duration of an individual pulse is ~700 zs rms.

*DJ Dunning, BWJ McNeil & NR Thompson, Phys. Rev. Lett. **110**, 104801 (2013)

High-Brightness SASE*

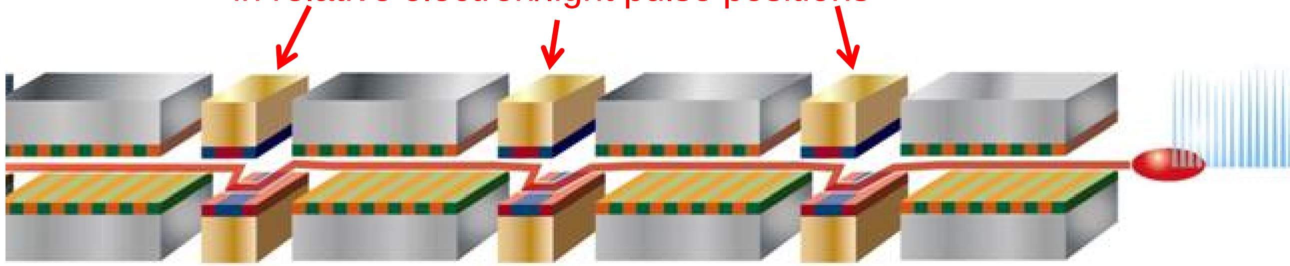

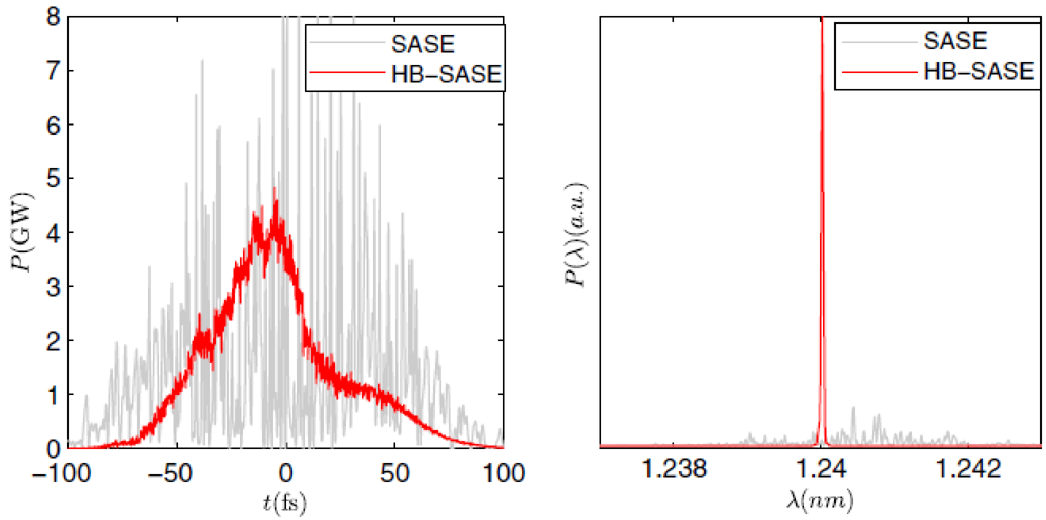

FIG. 4 (color online). Soft x-ray example at $\lambda_r = 1.24$ nm.

Greatly improved temporal coherence over SASE to give close to transform limited pulses in the hard x-ray

*BWJ McNeil, NR Thompson & DJ Dunning, Phys. Rev. Lett. **110**, 134802 (2013)

Some advantages of FELs

- Tuneable by varying electron energy or undulator parameters B_u and/or λ_u
- Spectral reach – THz, VUV to x-ray
- Cannot damage lasing medium (e^--beam)
- High peak powers (>GW's)
- Very bright (>~10^{30} ph/(s mm^2 mrad^2 0.1% B.W.))
- High average powers – 10kW at Jefferson
- Short pulses (<100*fs* → 100's *zs* (10^{-21}*s*))

The next generation of FELs will ensure that these sources are at the fore of light source provision for many years to come. Other sources are unable to meet all of the qualities of FELs by orders of magnitude in at least one respect.

Thank you!